The effect of crushing on the skid resistance of chipseal roads

R. Henderson, G. Cook, P. Cenek, J. Patrick, S. Potter
Opus Central Laboratories, Lower Hutt, New Zealand

Land Transport New Zealand Research Report 295

ISBN 0-478-28707-0
ISSN 1177-0600

PO Box 2840, Waterloo Quay, Wellington, New Zealand
Telephone 64-4-931 8700; Facsimile 64-4-931 8701
Email: *research@landtransport.govt.nz*
Website: *www.landtransport.govt.nz*

Henderson, R., Cook, G., Cenek, P., Patrick, J., Potter, S. 2006. The effect of crushing on the skid resistance of chipseal roads. *Land Transport New Zealand Research Report 295*. 132 pp.

Opus Central Laboratories, Opus International Consultants Ltd, PO Box 30 845, Gracefield, Lower Hutt

Keywords: aggregate, chipseal, crushing, macrotexture, microtexture, New Zealand, PSV, skid resistance, roads, traffic

An important note for the reader

The research detailed in this report was commissioned by Transfund New Zealand, and is published by Land Transport New Zealand.

Land Transport New Zealand is a Crown entity established under the Land Transport New Zealand Amendment Act 2004. The objective of Land Transport New Zealand is to allocate resources in a way that contributes to an integrated, safe, responsive and sustainable land transport system. Each year, Land Transport New Zealand invests a portion of its funds on research that contributes to this objective.

While this report is believed to be correct at the time of its publication, Land Transport New Zealand, and its employees and agents involved in its preparation and publication, cannot accept any liability for its contents or for any consequences arising from its use. People using the contents of the document, whether directly or indirectly, should apply and rely on their own skill and judgement. They should not rely on its contents in isolation from other sources of advice and information. If necessary, they should seek appropriate legal or other expert advice in relation to their own circumstances, and to the use of this report.

The material contained in this report is the output of research and should not be construed in any way as policy adopted by Land Transport New Zealand but may be used in the formulation of future policy.

Acknowledgments

The authors gratefully acknowledge the following quarries who supplied aggregate and information:

- Hastings Quarry, Holcim® Aggregates, Hastings;
- Pound Road Quarry, Fulton Hogan Limited, Canterbury.

In addition, the authors also extend thanks to the contributions of the peer-reviewers:

- Eric Souchon, President, Aggregate and Quarry Association of New Zealand (Inc.);
- Joanna Towler, Roading Engineer, Engineering Policy Section, Transit New Zealand.

Contents

Acknowledgments 4

Glossary 9

Executive Summary 13

Abstract 16

1. Introduction 17
- 1.1 Background 17
- 1.2 Objectives 17
- 1.3 Purpose of the Research 17
- 1.4 Report layout 18
  - 1.4.1 Key research activities 18
  - 1.4.2 Report outline 19
- 1.5 Background information and definitions 19
  - 1.5.1 Characteristics of greywacke alluvium 19
  - 1.5.2 Measurement of percent crushing 20
  - 1.5.3 Effects of percent crushing 20

2. Theory and measurement of skid resistance 21
- 2.1 Skid resistance theory 21
  - 2.1.1 Adhesion component of friction 21
  - 2.1.2 Hysteretic component of friction 22
- 2.2 Effect of slip speed 22
- 2.3 Wet versus dry skid resistance 22
- 2.4 Summary of observations 22
- 2.5 Skid resistance testers 23
  - 2.5.1 British Pendulum Tester 23
  - 2.5.2 GripTester 24
  - 2.5.3 SCRIM 25
  - 2.5.4 Correlation between skid testers 26

3. Aggregate polishing with the APM, and texture measurement techniques 27
- 3.1 The PSV test 27
  - 3.1.1 Accelerated Polishing Machine (APM) 28
  - 3.1.2 The British Pendulum Tester (BPT) in PSV mode 28
  - 3.1.3 Drawbacks of the PSV test 29
- 3.2 The Surtronic 3+ 30
  - 3.2.1 Surtronic 3+ 30
  - 3.2.2 Profile statistics 30
  - 3.2.3 Practical limitations 31
- 3.3 Transit NZ's Stationary Laser Profilometer (SLP) 31

4. Desk-top analysis of MSSC data 33
- 4.1 Investigation 1: Regional MSSC analysis 33
- 4.2 Investigation 2: Matched-pair MSSC analysis 34

5. Core samples for determining skid resistance 36
- 5.1 Core Samples 36
- 5.2 Measurements of skid resistance 36
  - 5.2.1 BPT measurements 37
  - 5.2.2 MSSC measurements 37

6. The PSV test 39
6.1 APM polishing 39
6.1.1 Test method 39
6.1.2 Results 39
6.1.3 Nominal PSV Values 41
6.1.4 Supplementary PSV Tests 41
6.2 Verification of APM-polishing 41
6.2.1 Test method 41
6.2.2 Results 42
7. Macrotexture polishing 44
7.1 Theoretical enveloping analysis 44
7.2 SLP analysis 45
8. GripTester and BPT friction measurements 46
8.1 Test surfaces 46
8.2 GripTester measurements 47
8.2.1 GripTester slip 47
8.2.2 GN' test procedure 48
8.2.3 GN' measurements 49
8.2.4 GN' results 50
8.3 BPN measurements 52
8.3.1 BPN tests on urethane-coated plates 52
8.3.2 BPN tests on uncoated plates 53
8.4 Discussion of GripTester and BPN test results 55
8.5 Comparison of GN' and BPN measurements 55
9. Relating skid resistance to percent crushing 56
9.1 Model construction 56
9.1.1 Effect of chip grade on BPN 56
9.1.2 Components of friction 56
9.2 Model calibration 57
9.3 Components of BPN friction 59
9.4 Model predictions for on-road terminally-polished chip 60
9.5 SFC predictions from BPN 61
9.6 Potential differences in predicted and actual skid resistance 62
10. Test procedures for relating skid resistance to percent crushing 63
10.1 Information required 63
10.2 Determination of microtexture 63
10.3 Determination of percent crushing 64
10.3.1 Initial comments 64
10.3.2 Angularity tests to determine percent crushing 64
10.4 Predictions 66
11. Other test procedures 67
11.1 Particle shape classification 67
11.2 SHRP angularity test procedures 67
11.3 Image-based particle shape classification procedures 67
11.4 Flow cone tests 69
11.5 Determination of macrotexture of existing roads using the SLP 70
12. Conclusions and recommendations 72
12.1 Conclusions 72
12.2 Recommendations 73
12.3 Analysis technique limitations 73
13. References 74
Standards 77

Appendices

1. Uncoated plates 81
2. Urethane-coated plates 87
3. PSV′ samples 91
4. Road core samples 93
5. Relationship between SLP profiles & percent crushing 99
6. Preparation & measurement for all tests 107
7. PSV microtexture profiles 109
8. Core sample selection 117
9. Core sample microtextures 119
10. GripTester measurements 121
11. Model development 123
12. Angularity test results 127
13. Microtexture statistics 129
14. Flow cone tests 131

Tables

1.1 Description of chapter contents. 19
3.1 Steps in the PSV test. 27
4.1 Site selection criteria for investigation 1. 33
4.2 Variation of MSSC by region. 34
4.3 Lane-km of aggregate used in Hawke's Bay and other RAMM geographic regions. 35
6.1 PSV′ results for APM-polished samples. 39
6.2 Nominal polished stone values. 41
6.3 Supplementary PSV′ tests with urethane-coated plates after 9 hours APM polishing. 41
6.4 Surtronic 3+ microtexture measurements of APM-polished samples. 42
6.5 Surtronic 3+ microtexture measurements of road-polished samples. 42
7.1 Analysis methods for SLP measurements. 45
8.1 Test plate data. 46
8.2 Test run data. 48
8.3 GripTester measurements. 49
8.4 BPN tests on urethane-coated plates. 51
8.5 BPN tests on urethane-coated chipseal plates. 52
8.6 BPN tests on new and uncoated chipseal plates (grades 2, 3 and 4). 53
9.1 Components of Equation 9.2. 56
9.2 Data for calculation of the constants in Table 9.3. 57
9.3 Constants for Equation 9.3. 58
9.4 Values to use in Equation 9.3 for on-road terminally-polished chipseal surfaces. 60
10.1 Test methods proposed for measuring parameters for estimating skid resistance variation... 63
11.1 Image indices. 67
11.2 Methods for predicting the percent crushing from SLP profiles. 71

Figures

2.1 Adhesion and hysteretic components of friction 21
2.2 British Pendulum Tester in use. 23
2.3 Diagram of the GripTester. 24
2.4 GripTester in 'tow' mode. 24
2.5 SCRIM truck. 25
2.6 Diagram of SCRIM skid resistance tester. 26
3.1 The Accelerated Polishing Machine used by Opus Central Laboratories. 28
3.2 British Pendulum Tester. 29
3.3 The Surtronic 3+ texture measurement instrument used by Opus Central Laboratories. 30
3.4 Transit NZ's SLP. 31
3.5 Example of an SLP profile. 32
5.1 Variation of MSSC' with HCV passes. 37
5.2 Variation of MSSC' with HCV passes. 38
6.1 Variation of PSV' with hours of polishing. 40
6.2 Comparison of APM-polished and HCV (road)-polished aggregates. 43
7.1 Predicted contact profile. 44
7.2 Predicted contact pressure. 44
8.1 GripTester measurements (operator's view). 48
8.2 Test plates showing wooden-inserts to reduce GripTester 'bounce'. 49
8.3 Variation of GN' with percent crushing. 51
8.4 Variation of BPN with percent crushing, urethane-coated plates. 53
8.5 Variation of BPN with percent crushing for new uncoated chip (R^2 = 0.997). 54
9.1 Variation of BPN: actual and predicted (Equation 9.3). 58
9.2 The components of BPN friction (Pound Road aggregate, new and unpolished). 59
9.3 Predicted variation of BPN: new and on-road terminally-polished aggregate. 61
9.4 Estimated variation of SFC with percent crushing. 62
10.1 Mass of compacted aggregate v percent crushing (Hastings Quarry). 65
10.2 Mass of compacted aggregate v percent crushing (Pound Road Quarry). 65
10.3 Mass of compacted aggregate v percent crushing (Pound Road Quarry). 65
11.1 Funnel for flow cone tests. 69

Glossary

Abbreviations

Abbreviation	Meaning
AADT	Average Annual Daily Traffic
AAV	Aggregate Abrasion Value (BS 812, Part 113:1990)
ABS	Anti-lock Braking System
ACV	Aggregate Crushing Value (BS 812, Part 113:1990)
AIV	Aggregate Impact Value (BS 812, Part 113:1990)
ALD	Aggregate Least Dimension
APM	Accelerated Polishing Machine (BS 812, Part 114:1989)
Alluvial	Transported by river
Asperity	A sharp irregularity on the surface of the pavement surface that is expected to contact the tyre
Assessment length L_n	
ASCE	American Society of Civil Engineers
ASME	American Society of Mechanical Engineers
ASTM	American Society for Testing and Materials: a voluntary Standards organisation based in Pennsylvania, US
Barmac	Type of aggregate crusher
BPN	British Pendulum Number (BS EN 13036, Part 4:2003)
BPT	British Pendulum Tester, also called the Pendulum Friction Tester (BS EN 13036, Part 4:2003)
BWP	Between wheelpaths
Comminution	The process of crushing and/or grinding raw aggregate
Cone	Type of aggregate crusher
Cut-off length	L_c (= Sampling length)
Enveloping	The process whereby a tyre contacts only the upper part of a road profile
ESC	Equilibrium SCRIM Coefficient: ESC is MSSC data smoothed for year-to-year variations; the RAMM database from 2002 onwards is populated with ESC data
Evaluation length L_n	
Form	A measure of the overall proportions of a particle; Form is most commonly measured as sphericity which is the volume of the particle divided by the volume of a circumscribing sphere
GN	GripNumber
GN´	Modified GripNumber (the GripNumber obtained using (a) the GripTester in 'push' mode and (b) narrow test plates for the measurement wheel only)
Gravel	Unconsolidated rock between 2 mm and 75 mm in size: it can be crushed or uncrushed
GripNumber	The skid resistance number reported by the GripTester
GripTester	A fixed-slip friction measuring machine
HCV	Heavy Commercial Vehicle
HCV polishing	Polishing of road surfaces by heavy commercial vehicle tyres
HMA	Hot Mix Asphalt
IFI	International Friction Index as per ASTM E-1960-98: *Standard Practice for Calculating International Friction Index of a Pavement Surface*

LWB	Locked wheel braking: the value of skid resistance measured by locked wheel braking tests using a vehicle (in which the test vehicle decelerates to rest by locking the wheels)
Macrotexture	Pavement texture with a wavelength 0.5-50 mm
Megatexture	Pavement texture with a wavelength 50-500 mm
Microtexture	Aggregate texture with a wavelength less than 0.5 mm
MPD	Mean Profile Depth (mm): a laser-based texture depth measure as per ISO 13473-1:1996
MTD	Mean Texture Depth (mm): texture depth determined by the Sand Patch Method (BS 598, Part 105:2000)
MSSC	Mean Summer SCRIM Coefficient: previously called NZMSSC in RAMM, is the mean SCRIM coefficient over the summer period when skid resistance is generally at its lowest
MSSC'	MSSC averaged over three years to reduce seasonal fluctuations
OWP	Over wheelpath
Pea-gravel	Uncrushed alluvial aggregate, dominantly of gravel size (2–76 mm)
PIARC	The World Road Association, a non-political and non-profit making association
PFT	Pendulum Friction Tester, also called the British Pendulum Tester (BS EN 13036, Part 4:2003)
Percent slip	Tyre slip speed as a percentage of vehicle speed: 0% slip corresponds to a free-rolling tyre, and 100% slip corresponds to locked-wheel braking (i.e. sliding speed = vehicle speed)
PSD	Power Spectral Density: PSD can be thought of as the energy content of a profile (proportional to m^2) as a function of spatial frequency (1/m), and therefore has units (m^2 per 1/m)
PSV	Polished Stone Value (BS 812, Part 114:1989)
PSV_0	PSV' for pea-gravel
PSV_{100}	PSV' for sealing chip
PSV'	The PSV obtained with a standard PSV test with the following changes: 1. One APM-polishing run completed instead of two; 2. No corrections made according to the PSV of the control stone
PSV_{raw}	Uncorrected (raw) Polished Stone Value
RAMM	Road Assessment and Maintenance Management database
Road polishing	Polishing of road surfaces by traffic tyres (especially HCV)
Roundness	A measure of the sharpness of chip corners
RS	Reference Station
Sampling length	L_C (= Cut-off length)
Sealing chip	Aggregate suitable for constructing chipseal pavements according to Transit New Zealand's document M/6:2004 *Specification for Sealing Chip*
SCRIM	Sideways Force Coefficient Routine Inspection Machine (BS 7941, Part 1:1999), Figure 2.6
SFC	Sideways Force Coefficient: the friction coefficient measured by the SCRIM
SH	State Highway
SHRP	Strategic Highway Research Program: a research program implemented in the US, active from 1988-1993
SLP	Stationary Laser Profiler
Slip speed	The speed of sliding between a tyre and pavement
Surface texture	Another term for macrotexture

Sphericity	The volume of the particle divided by the volume of a circumscribing sphere
Terminal state of polish	The equilibrium or ultimate state of polish
TNZ	Transit New Zealand, responsible for NZ state highways
TRL	Transport Research Laboratory, UK (pre-1992)
TRRL	Transport Road Research Laboratory, UK (1992 onwards)
UK	United Kingdom
US	United States of America

Units

g	grams
kg	kilograms
kHz	kilohertz (10^3 samples/second)
km	kilometres
km/h	kilometres per hour
m	metres
kPa	kilopascals (10^3 Pa)
MPa	Megapascals (10^6 Pa)
Pa	Pascals ($\equiv N/m^2$)
um	micro-metres (10^{-6}m)
μm	micro-metres (10^{-6}m)
	(Note: sometimes 'μm' is written as 'um' on graphs due to font limitations with software packages)

Symbols

C	The mean of the PSV_{raw} for four control specimens (two from each run)
d	Cone outlet diameter (mm)
F	Friction
F_a	Adhesion component of friction
F_h	Hysteretic component of friction
F_v	Viscous component of friction
F_t	Tearing component of friction
L	Traverse length (= profile length in the absence of filtering)
L_c	Cut-off or sampling length
L_n	Evaluation or assessment length (= traverse length in the absence of filtering)
M	Mass of compacted aggregate (g)
M_f	Load on each treaded front wheel of GripTester
M_m	Load on measurement wheel of GripTester
N	Number of sampling lengths per assessment length (L_n/L_c): the default value is 5
R	Correlation coefficient
R_a	Roughness average as per ASME Y14.36M-1996
S	The mean value of the PSV_{raw} for four test specimens (two from each run)
Ø	Diameter

Subscripts

f	Front wheels of GripTester
m	Measurement wheel of GripTester
a	Adhesion
h	Hysteresis
v	Viscous
t	Tearing
c	Cut-off or sampling
n	Evaluation or assessment

Conventions

Unless otherwise stated, linear lines on graphs are fitted to data using the least squares technique.

Transit New Zealand's definition of 'broken faces' is not explicitly used. Instead, the term 'percent crushing' is more appropriate for work undertaken in this research and is generally used in this report. Further explanation of this is given in Section 1.5.2.

Executive summary

This research was carried out between 2003 and 2005 at Opus International Consultants, Central Laboratories, Lower Hutt.

Background

The relationship between (a) aggregate microtexture, (b) percentage of crushed faces, (c) chip shape, and (d) skid resistance is not well understood. For example, Transit New Zealand (TNZ) has proposed that future TNZ M/6 sealing chip specifications include a new definition of broken faces that will require a significant increase in the percentage of crushed faces of processed aggregate. Depending on the microtexture of the particular aggregate, this requirement may not always be necessary to achieve skid resistance criteria.

Objectives

The objectives of this research project were to:

1. Allow more effective utilisation of road surfacing aggregate by better understanding how aggregate shape and texture affect skid resistance.
2. To determine the effect of broken faces on the skid resistance of aggregates.

As part of meeting these objectives, this research project has sought to answer the following questions:

1. What microtexture and shape parameters contribute to a high skid resistance?
2. Can an aggregate with low microtexture provide acceptable skid resistance by giving it a high percentage of broken faces? Or, if an alluvial aggregate has a high microtexture, can it have fewer broken faces (i.e. less crushing)?
3. What influence does chip size have on skid resistance?

Research Activities

This research has focused on aggregate sourced from two quarries, both of which use alluvial greywacke aggregate:

- Hastings Quarry, Holcim® Aggregates, Hastings;
- Pound Road Quarry, Fulton Hogan Limited, Canterbury.

The research comprised the following key activities:

- Comparison of the polishing action employed in the Polished Stone Value (PSV) test with actual polishing on roads.
- GripTester and British Pendulum Tester tests on laboratory-prepared chipseal plates to determine the effect of crushing on skid resistance.
- Assessment of test procedures for determining chip shape and the percentage of crushing.

- Development of a model to estimate the relationship between friction and the percentage of crushed chips.

Conclusions

The results of PSV, GripTester and BPT tests on core samples and laboratory-prepared chipseal surfaces from two quarries using greywacke indicate that:

- Skid resistance increases linearly with percentage crushing. For new and unpolished aggregate, the increase in BPN in going from 0% crushed chips to 100% crushed chips is approximately 25%.
- Skid resistance increases with crushing by two mechanisms:
  - The microtexture of crushed faces is greater than the microtexture of uncrushed faces (after Accelerated Polishing Machine (APM) polishing, the increase in PSV of crushed faces compared with uncrushed faces is approximately 4.5 PSV units).
  - New and unpolished crushed chips are more 'angular' in shape than uncrushed chips, but for heavily polished surfaces where sharp chip edges have become rounded, the increase in BPN due to chip shape in going from 0% crushed chips to 100% crushed chips is estimated as negligible.
- The increase in skid resistance caused by crushing results mainly from (a) the increased microtexture of crushed faces rather than (b) the 'angular' shape of crushed chips (e.g. for new and unpolished chip, the increase in BPN in going from 0% to 100% crushed chips is 19% related to microtexture increases, and 7% related to increases chip shape 'angularity').
- BPN is not noticeably affected by chip size (i.e. by chip grade).
- The degree of crushing required to meet a particular level of skid resistance depends on both uncrushed and crushed (a) microtexture, and (b) chip shape.
- Aggregates with a lower level of microtexture need to be crushed more to achieve a given level of skid resistance (e.g. new and unpolished aggregate with a PSV of 55 needs 100% crushed chips to achieve the same skid resistance as aggregate with a PSV of 57 that has 88% crushed chips). (Skid resistance is measured by GripNumber in 'push' mode, i.e. GN´.)
- For aggregates with the same microtexture, chips that have 'irregular' shapes have greater BPN than 'round' chips (e.g. when 100% crushed, the BPN of 'irregular' chips is greater than that of 'rounded' chips by approximately 9 BPN).
- The benefit of crushing on skid resistance is greater for new and unpolished chipseal surfaces than for terminally-polished chipseal surfaces. Polishing reduces the benefit of crushing on skid resistance by (a) reducing the microtexture of crushed faces, and (b) 'smoothing' sharp chip edges that were angular when first produced.
- The beneficial effect of crushing on microtexture remains after the equilibrium level of polish is achieved. (The increase in PSV when 100% crushed chips are used

instead of 0% crushed chips is between 10 and 15 for unpolished chips, but this reduces to between 4 and 5 PSV after PSV polishing.)

- Sharp or angular asperities at the edges of chip faces on new and unpolished chip become rounded with polishing by Heavy Commercial Vehicles (HCVs).
- When operated on low-friction surfaces, the GripTester in 'push' mode gives different trends of skid resistance than the British Pendulum Tester.
- The test specified by the British Standard *Determination of angularity number* (BS 812: Part 1:1975, 7.5) would appear useful for determining the percentage of crushed chips. (Such a test may also be useful for quantifying chip shape, although this has not been investigated as part of this research.)

Recommendations

- Further develop and validate the conclusions above using:
  - Aggregate from additional quarries.
  - On-road skid resistance measurements using the GripTester in 'tow' mode on a range of specifically constructed chipseal surfaces with a range of percentage of crushed chips (e.g. 0%, 50%, 80%, and 100%).
- Further investigate the test method of BS 812: Part 1:1975, 7.5 to quantify the shape of aggregate chips and so enable the contribution of chip shape to skid resistance to be accurately predicted.
- A survey of crushing methods employed by New Zealand sealing chip suppliers be undertaken. This survey should aim to determine how the method of crushing (e.g. Barmac, Cone, etc.) affects aggregate shape.

Analysis Technique Limitations

- Analysis of the microtexture profiles of aggregate measured using an instrument such as the stylus-based Surtronic 3+ has not been useful in this research.
- It has not been possible in this research to accurately compare the polishing employed in the PSV test with actual polishing of tyres on the road. Consequently, it has not been possible to validate (or otherwise) the polishing action employed in the PSV test.
- It has not been possible in this research to distinguish the percentage of crushed faces in existing surfaces with analysis of Stationary Laser Profiler (SLP) profiles.
- Image-based shape classification techniques at the time of preparing this report are useful only as research tools and have not been developed to the point where they can be used in laboratory test procedures.

Abstract

This research was carried out between 2003 and 2005 at Opus International Consultants, Central Laboratories, Lower Hutt. Research has focused on chipseal surfaces constructed using greywacke aggregate from two quarries.

This research was to determine the relationships between (a) aggregate microtexture, (b) percentage of crushed faces, (c) chip shape, and (d) skid resistance with the main focus being on determining the effect of crushing on skid resistance. The PSV, GripNumber and British Pendulum Number (BPN) results from core samples and laboratory-prepared chipseal surfaces that show the relationships are presented.

1. Introduction

1.1 Background

The relationship between (a) aggregate microtexture, (b) percentage of crushed faces, (c) chip shape, and (d) skid resistance is not well understood. For example, Transit New Zealand (TNZ) has proposed that future TNZ M/6 sealing chip specifications include a new definition of broken faces that will require a significant increase in the percentage of crushed faces of processed aggregate.

Depending on the microtexture of the particular aggregate, this requirement may not always be necessary to achieve skid resistance criteria. For example, adequate skid resistance is measured by annual SCRIM surveys on Canterbury roads where semi-crushed alluvial aggregate with a low percentage of broken faces has traditionally been used. The proposed change to the requirements would considerably affect the New Zealand aggregate market, and create a resource and economic problem in regions that rely predominantly on alluvial aggregate suppliers (e.g. Canterbury, Manawatu).

1.2 Objectives

The objectives of this research project were to:

1. allow more effective utilisation of road surfacing aggregate by better understanding how aggregate shape and texture affect skid resistance;
2. determine the effect of broken faces on the skid resistance of aggregates.

1.3 Purpose of the Research

Given the lack of information on the effect of aggregate texture and shape characteristics on skid resistance, accurate decisions on the degree of crushing needed for a particular aggregate to meet skid resistance criteria cannot be made.

This research project has sought to answer the following questions:

1. What microtexture and shape parameters contribute to a high skid resistance?
2. Can an aggregate with low microtexture provide acceptable skid resistance by giving it a high percentage of broken faces? Or, if an alluvial aggregate has a high microtexture, can it have fewer broken faces (i.e. less crushing)?
3. What influence does chip size have on skid resistance?

A key change over earlier work (e.g. Cenek et al. 1998) is that aggregate microtexture, previously assessed qualitatively with binocular microscopy, is measured directly and quantitatively with the Opus stylus profilometer.

While international research over the past 30 years has developed models for predicting skid resistance from pavement texture, these tend to be relatively simple empirical models that often do not give good predictions of skid resistance. Reasons include (a) failure to isolate the portion of texture that is in contact with the tyre (enveloping), and (b) lack of ability to accurately measure microtexture profiles. In addition, some models were developed from measurements taken on smooth concrete pavements and runways, and these cannot be successfully applied to the rough-surfaced chipseal pavements used in New Zealand.

All the field and laboratory work undertaken for this report used greywacke aggregate from the following two quarries:

1. Hastings Quarry, Holcim® Aggregates, Hastings;
2. Pound Road Quarry, Fulton Hogan Limited, Canterbury.

The decision to concentrate on aggregate from these two quarries was made because:

1. The two quarries in question both use alluvial greywacke aggregate.
2. Roading aggregate from quarries in Canterbury is reportedly 'harder' than aggregate used in some other regions, including Hawke's Bay.
3. Roading aggregate from quarries in Canterbury reportedly have greater microtexture when polished than aggregate from Hastings. (The polished stone values (PSVs) of the aggregate from the two quarries are 57 and 55 respectively.)
4. Roads in the Canterbury region generally have adequate skid resistance when measured by Transit NZ's annual SCRIM surveys. This has not always been true of roads in the Hawke's Bay region in the past.
5. For a given region, direct comparisons could be made between PSV-polished and road-polished cores because the aggregates were from the same quarries.

While using aggregate from a hard-rock quarry as a control was considered, this was not done as aggregate from hard-rock quarries is available only in the crushed form, not as pea-gravel[1]. This would mean that experimental studies looking at the effect of percentage crushing on skid resistance using aggregate from hard-rock quarries would be difficult.

1.4 Report layout

1.4.1 Key research activities

The key research activities were:

Key 1: Comparison of the polishing action of vehicle tyres with that employed in the PSV test (Chapter 6).

Key 2: GripTester and British Pendulum Tester (BPT) tests to determine the effect of percent crushing on skid resistance (Chapter 8).

[1] Pea-gravel – uncrushed alluvial aggregate, dominantly of gravel size (2–76 mm).
Gravel – unconsolidated rock between 2 mm and 75 mm in size: it can be crushed or uncrushed

Key 3: Development of a model to relate percentage of crushing to friction (Chapter 9).

Key 4 Assessing test procedures for determining chip shape and percent crushing (Chapters 10 and 11).

1.4.2 Report outline

The contents of each chapter in this report are summarised in Table 1.1.

Table 1.1 Description of chapter contents.

Chapter	Description of Contents
2	Backgrounds skid resistance theory, focusing on the adhesion and hysteretic components of friction, and describes skid resistance testers used in this research (i.e. the BPT, the GripTester and SCRIM).
3	Details the PSV test and equipment, and texture measurement instruments (the Surtronic for microtexture, and TNZ's SLP for macrotexture) used in this research.
4	Describes results of a desktop study of skid resistance values measured by SCRIM for aggregate from the same regions as that used in Chapters 5-11 of this study.
5	Describes results of skid resistance tests (both BPT and SCRIM) on road core samples.
6	Outlines the results of verification tests comparing the polishing employed in the PSV test with polishing by traffic tyres.
7	Summarises SLP measurements to determine the road surface profile changes caused by traffic polishing.
8	Details GripTester and BPT measurements to determine the effect of percent crushing on skid resistance.
9	Details the development of a model to predict skid resistance based on PSV measurements and percent crushing.
10	Gives test procedures for determining the variables suitable for employing in skid resistance prediction model of Chapter 9.
11	Details other test procedures, including optical shape measurements procedures, flow-cone measurements of inter-particle friction, and SLP tests to estimate the percentage of crushing of an existing chipseal surface.

1.5 Background information and definitions

1.5.1 Characteristics of greywacke alluvium

Approximately three-quarters of New Zealand quarries supplying sealing chip produce aggregate from greywacke deposits. This is true of both hard-rock and alluvial quarries. Other rock types for sealing chip include andesite and basalt, both from hard-rock sources (G. Cook 2003, pers.comm.).

Greywackes are sandy and are a class of sandstone, i.e. a sedimentary rock. In colour, greywackes are generally dull and grey, brown, yellow or black. The grains are predominantly quartz, and to a lesser extent feldspar, with sub-angular and angular particles of other minerals. The grain size is typically from 0.06 to 2.0 mm (Fookes et al. 2001) with the matrix being fine clay and generally constituting more than 15% of the rock by volume (The Encyclopedia Britannica 2005).

1.5.2 Measurement of percent crushing

In this research report, the definition used by Transit NZ to define 'broken faces' has not generally been employed, and instead definitions are in terms of 'percent crushing'. This decision was made primarily to make laboratory tests more rapid and cost-effective. 'Percent crushing' was defined as the ratio by weight of sealing chip:pea-gravel multiplied by 100. Before combination, both the sealing chip and pea-gravel were washed, oven-dried at 105°C for 12 hours, and sieved.

The following errors are inherent in the approach taken:

1. Sealing chip is not 100% crushed. (Assuming the supplied samples of sealing chip met the specification of TNZ M/6, at least 98% of the chips had two or more broken faces. Visually, the sealing chip samples appeared to be essentially 100% crushed.)
2. Pea-gravel may not always be completely uncrushed, with occasional crushed faces resulting from natural crushing. (Observations were that a chip of pea-gravel sometimes split along a seam. Visually, the percentage of crushed chip in a pea-gravel sample was minimal, and is estimated at less than 1%.)
3. The size distribution of sealing chip and pea-gravel may not be the same. (Efforts were taken to minimise this by (a) sieving the supplied aggregate samples before use, and (b) ensuring that approximately equal quantities of rejected chip was oversize ('held' when sieved) or undersize ('passed' when sieved)).

The errors associated with the approach taken are not believed to influence the research findings and the 'percent crushing' definition used here is believed to be practical and usable by both quarries and laboratories.

1.5.3 Effects of percent crushing

For hot mix asphalt (HMA) surfaces, crushing aggregate reduces rutting because the internal friction between particles is higher (Minnesota DoT 2003).

For chipseal surfaces, crushing aggregate can be expected to increase skid resistance by two mechanisms:

1. Crushed faces have increased microtexture.
2. Crushing changes the shape of chips from 'rounded' to 'angular'.

As far as the authors of this report are aware, these benefits, although reasonably well established in descriptive terms, have not been accurately quantified.

2. Theory and measurement of skid resistance

2.1 Skid resistance theory

According to research papers by both French (1989) and Clark (1981), the total friction force between a road surface and tyre can be expressed as:

$$F = F_a + F_h + F_v + F_t \qquad \text{Equation 2.1}$$

where:

- F = Total friction force between the road surface and tyre
- F_a = Adhesion component of friction
- F_h = Hysteretic component of friction
- F_v = Viscous component of friction
- F_t = Tearing component of friction

Of the four components of friction, only adhesion friction (F_a) and hysteretic friction (F_h) are significant in magnitude (Moore 1975) and will be considered in this report. While published research is somewhat inconclusive in terms of quantitative analysis, the adhesion component of friction (F_a) is generally regarded as making the largest contribution to friction and the hysteretic component (F_h) less (e.g. 20%) of the total friction (Anderson & Henry 1979).

Figure 2.1 shows a diagram of the mechanisms of adhesion and hysteretic components of friction in schematic form.

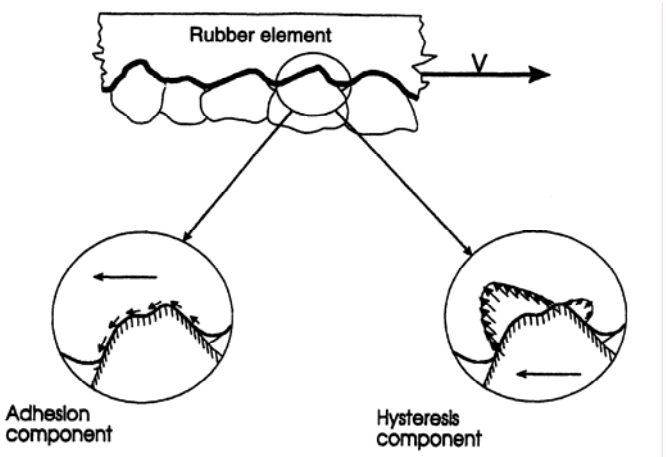

Figure 2.1 Adhesion and hysteretic components of friction (Choubane et al. 2004).

2.1.1 Adhesion component of friction

The adhesion component of friction results from inter-molecular attraction between the tread rubber of tyres and aggregate chips. For perfectly dry surfaces, maximum adhesion is obtained for flat and smooth surfaces. For wetted surfaces, adhesion friction rises with microtexture, with the microtexture asperities 'piercing' the water film and providing dry pavement–tyre contact regions (Moore 1975).

2.1.2 Hysteretic component of friction

The hysteretic component of friction results from deformation of the tread rubber as it contacts macrotexture asperities. Damping in the rubber means that not all of the energy absorbed in deforming the rubber is returned when the tread rubber returns again to its undeformed state (Clark 1981). As shown in the diagram in the right-hand circle of Figure 2.1, this results in a horizontal component force which acts in the opposite direction to tyre movement. This component of friction is small in free-rolling wheel rotation, but significant for locked-wheel braking (Moore 1975) because of the increased rubber deformation that occurs when sliding rather than rolling. Hysteretic friction would be expected to increase with chip irregularity as 'angular' chips cause more deformation of the tread rubber than 'rounded' chips.

2.2 Effect of slip speed

Because the hysteretic component of friction increases with percent slip, the proportion of hysteretic friction compared to the total friction would be expected to increase with percent slip. This contributes to the phenomenon where skid testers with different percentages of slip predict different levels of friction.

2.3 Wet versus dry skid resistance

Additional to the discussion above, wet skid resistance is less than the skid resistance for dry tyre–road contact, principally because the adhesion component of friction is reduced. Ensuring adequate wet skid resistance requires that adequate macrotexture is available for water drainage (Mooney & Wood 1996) with the major role of macrotexture being to provide drainage paths for the water, and allow penetration of the tyre through the water film to contact the pavement. This forms a so-called 'dry contact region' (Horne & Buhlmann 1981).

With all the skid testers mentioned in this report, water was applied to the pavement surface before skid resistance measurements were made.

2.4 Summary of observations

From the discussion in Sections 2.1–2.3, three observations can be made:

1. The adhesion component of friction on a wetted surface increases with microtexture.
2. The hysteretic component of friction increases with chip angularity.
3. The hysteretic component of friction increases from a minimum for a free-rolling tyre to a maximum at 100% slip.

2.5 Skid resistance testers

The following pavement friction testers were used in the testing undertaken as part of this research. They are explained briefly in the text below.

2.5.1 British Pendulum Tester

Sliding Speed: 10 km/h

The Pendulum Friction Tester (BPT) was developed by the Transport & Road Research Laboratory (TRRL), Department of Scientific and Industrial Research, UK. The friction measured by the BPT is intended to correlate with the performance of a vehicle with patterned tyres braking with locked wheels on a wet road at 50 km/h.

Figure 2.2 British Pendulum Tester in use.

The instrument utilises a rubber slider mounted to the end of a pendulum arm. The amount of energy absorbed by the rubber slider passing over the test surface is reflected in the angle of the pendulum arm at the end of its stroke: the smaller the arc of swing, the greater the energy absorbed by slider-pavement friction. A graduated scale and pointer provides a numerical measure of friction.

The instrument can be used to provide a measure of friction either in the field or in the laboratory, and emphasises the contribution to friction of microtexture rather than macrotexture. The instrument cannot be used to measure the friction of very coarse irregular surfaces (i.e. a rough macrotexture) because the length of the pendulum arm has to be adjusted to obtain the specified contact length between the slider and test surface. Coarse chipseals (e.g. grade 2) are often difficult and time-consuming to measure for this reason.

2.5.2 GripTester

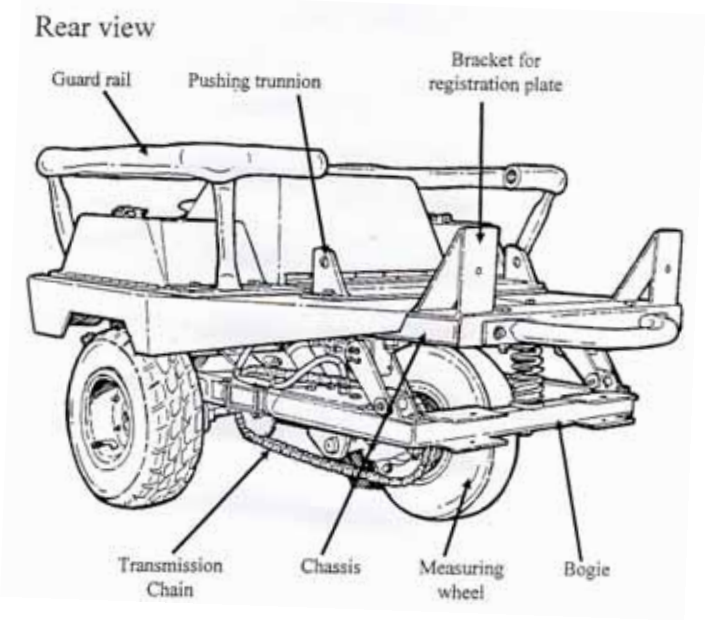

Figure 2.3 Diagram of the GripTester.

The GripTester (Figure 2.3) is a fixed-slip skid tester and has tyres in a tricycle arrangement: two treaded 10" (inch) diameter drive tyres at the front of the unit, and one 10" diameter untreaded tyre at the rear of the unit for skid resistance measurement (labelled the 'Measuring wheel'). The measuring wheel rotates with 15% slip on the test surface via a chain drive connected to the drive wheels. Load cells measure the horizontal and vertical forces on the measurements wheel and the ratio is the reported friction.

Figure 2.4 GripTester in 'tow' mode.

The GripTester can be used in 'tow' mode at typical vehicle speeds (Figure 2.4), or in 'push' mode at walking speed. For the 'tow' mode configuration, water is applied to the road from a tank mounted in the back of the towing vehicle, and from a hand sprayer or similar in 'push' mode.

Percent slip:	15%
Survey Speed:	Vehicle speed in 'tow' mode
	Walking speed in 'push' mode (~5 km/h)
Slip Speed:	0.75 km/h in 'push' mode (i.e. 15% of 5 km/h)
Weight on Measurement Wheel:	22 kg
Total weight:	85 kg

2.5.3 SCRIM

Figure 2.5 SCRIM truck.

The SCRIM (Sideways Force Coefficient Routine Inspection Machine, Figure 2.5) travels at vehicle speed and is suitable for surveying up to approximately 250 km/day. A SCRIM measurement truck has been used by Transit NZ for their surveys of the skid resistance of the State Highway (SH) network since 1995, and annually since 1998. Results are available in the RAMM (Road Assessment and Maintenance Management) database as ESC (Equilibrium SCRIM Coefficient), MSSC (Mean Summer SCRIM Coefficient), and the SCRIM coefficient.

SCRIM is an example of a side force skid tester and utilises an untreaded measurement wheel mounted at 20° to the direction of travel. Water is applied to the road surface from a 2750 litre storage tank (Figure 2.6).

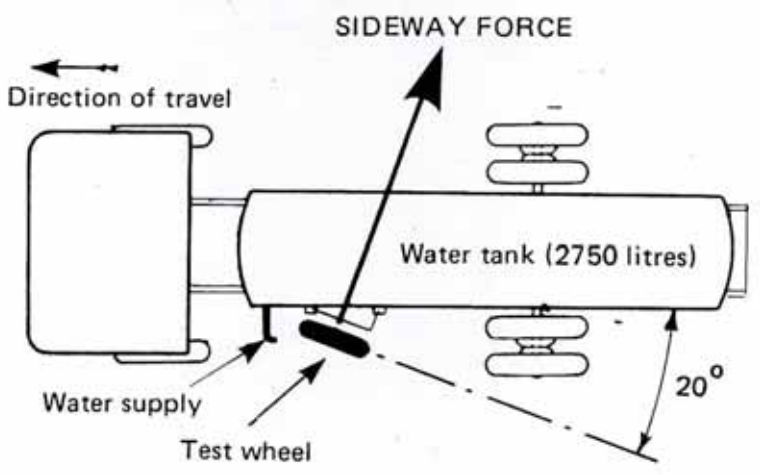

Figure 2.6 Diagram of SCRIM skid resistance tester.

Survey Speed:	Typically 50-80 km/h
Angle of Test Wheel:	20° to direction of travel
Slip Speed:	17.1 km/h at survey speed of 50 km/h (50×sin(20°))
Percent Slip:	34.2% (i.e. 100×sin(20°))
Test wheel size:	76 mm wide × Ø508 mm
Tyre pressure:	350 kPa (50.8 psi)
Tyre rubber:	Resilience and hardness standardised
Test wheel load:	200 kg

2.5.4 Correlation between skid testers

Correlations between the friction measures provided by the BPT, the GripTester and SCRIM are good (Cenek et al. 2004) and conversion between friction measurements made with these three devices can be achieved with the use of the relations developed by PIARC (1995). While these measurements will not necessarily represent the braking performance for a specific vehicle (e.g. for accident investigation purposes), they are very useful for the investigation and management of the skid resistance on roads. The actual friction experienced by a car performing locked-wheel emergency braking will be a function of, in addition to the road surface, the following:

1. Sliding speed
2. Inflation pressure of the tyre
3. Tread pattern
4. Lubricating effect of tyre rubber deposited on the road
5. Temperature
6. Water film thickness
7. Other factors

This list has been compiled by the authors.

3. Aggregate polishing with the APM, and texture measurement techniques

Two methods have been used in this research to determine the microtexture of polished aggregate:

(a) an indirect method using PSV (Section 3.1), and

(b) a direct method using a Surtronic 3+ stylus profilometer (Section 3.2).

Accurate determination of the microtexture of polished aggregate was considered necessary to:

(a) properly assess any difference in microtexture between quarries and between crushed/uncrushed aggregate, and

(b) evaluate the polishing action employed in the PSV test.

The Stationary Laser Profiler (SLP) has been used to quantitatively assess the macrotexture of aggregate. It is described briefly in Section 3.3.

3.1 The PSV test

The PSV test is intended to rank aggregates according to their susceptibility to polish under the action of traffic. In New Zealand, aggregates used for roads typically have PSV which range from 51 to 65, with greywacke aggregate having a typical value of approximately 57. Six hours of aggregate polishing is assumed to be sufficient to achieve a so-called 'ultimate', 'terminal', or 'equilibrium' state of polish. This has been borne out by the research described here (Figure 6.1), but other authors in different countries report that some aggregates continue to polish well after the standard 6-hour test period has elapsed (e.g. Perry et al. 2001). While the PSV primarily is intended to rank aggregates according to how they polish, the PSV can also be regarded as a surrogate measure of friction of an aggregate in the polished state. A PSV test involves 3 steps, which are summarised briefly in Table 3.1.

Table 3.1 Steps in the PSV test.

Step	Activity	Description
1	Sample Preparation	Curved samples are prepared using 10 mm chips. The samples have translucent resin backs and special moulds are used to ensure that the samples are of the correct size and shape to fit the Accelerated Polishing Machine (APM) test wheel (Figure 3.1). When preparing the samples, aggregates are arranged to expose flat surfaces, rather than irregular surfaces with asperities. The actual plates used in this research project are shown in Appendix 3.
2	Polishing (Figure 3.1)	Polishing is achieved with the APM (Figure 3.1). This process is described further in Section 3.1.1.
3	Friction Testing (Figure 3.2)	Friction testing is achieved with the BPT, especially configured for a PSV test described in Section 3.1.2.

3.1.1 Accelerated Polishing Machine (APM)

Figure 3.1 The Accelerated Polishing Machine used by Opus Central Laboratories.

The APM consists of a large wheel which carries the samples, and a smaller solid rubber tyre with a 725 N load. Abrasive slurry is fed between the solid rubber tyre and samples to polish the aggregate. For the first three hours, the abrasive slurry consists of emery grit and water, and for the second three hours the slurry consists of emery flour and water. The grit and flour are fed onto the samples via a toothed belt from hoppers positioned on top of the machine. In total, 115,200 rotations of the large wheel are completed in a standard PSV test.

In a standard PSV test, a minimum of two sample plates are tested in the first run, and a further two plates in a second run. In both cases, a control aggregate is assessed in every run to correct for minor fluctuations in polishing conditions, and to improve the repeatability and reproducibility of the test.

3.1.2 The British Pendulum Tester (BPT) in PSV mode

Figure 3.2 shows the equipment used for PSV friction measurements. The technique is the same as that employed in a standard British Pendulum Number (BPN) test of a road surface, except that:

1. a special narrow rubber slider replaces the standard wider rubber slider;
2. a dedicated PSV scale is used.

Figure 3.2 British Pendulum Tester.
(from http://www.rjmaxwell.com/education/aggregate_tests)

3. PSV values are corrected according to results from a control stone according to the following formula:

$$PSV = S + (52.5 - C) \qquad \text{Equation 3.1}$$

where:

PSV = Polished Stone Value
S = Mean value of the PSV_{raw} for four test specimens (two from each run)
C = Mean of the PSV_{raw} for four control specimens (two from each run)

3.1.3 Drawbacks of the PSV test

Drawbacks of using the PSV test to rank how aggregates would be expected to polish in the field include:

- The polishing caused by environmental effects, principally temperature and wetting/drying cycles, are not modelled by the PSV test.
- PSV can correlate poorly with SFC for some aggregates (Cenek et al. 2004).
- Some aggregates do not reach an equilibrium state of polish in the 6-hour duration of a standard PSV test (Perry et al. 2001).
- Some aggregates polish differently depending on the stress between the samples and loaded rubber wheel (for a PSV test) or between tyres and the surface (in the field). This is covered in detail by Perry et al. (2001).

3.2 The Surtronic 3+

3.2.1 Surtronic 3+

The Surtronic 3+ (Taylor Hobson 1993) is an instrument for measuring surface texture (Figure 3.3). It is portable and generally used for measuring the surface roughness of machined metal components. It is suitable also for measuring similarly rough surfaces on other hard materials. For measurement, it uses a diamond-tipped stylus (radius = 5.0 μm) which traverses the profile of the surface to be tested. The deflection of the stylus is sensed by an inductive pickup which produces an output in relation to stylus deflection. For protection, the arm is housed in a hollow outer tube (pickup rod).

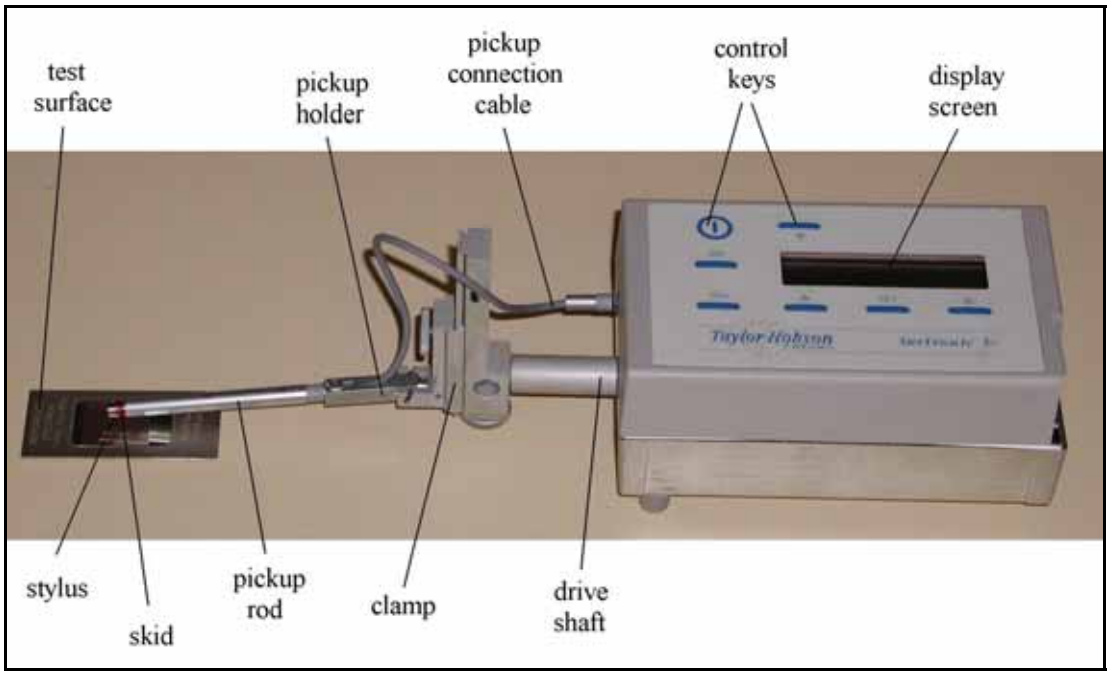

Figure 3.3 The Surtronic 3+ texture measurement instrument used by Opus Central Laboratories.

A drive motor is used to control movement of the stylus across the test surface via a linear drive shaft. A membrane type push-button control is used with a monochrome liquid crystal display screen.

3.2.2 Profile statistics

For this project, standard texture statistics have been calculated for the profiles measured by the Surtronic 3+ using Matlab®, release 14. The statistics are detailed by Cenek et al. (2004) and are covered by the ISO Standards 4287/1:1984, 4287:1997, 13565-1:1996, 13565-2:1996 and ASME Standards B46.1:1985, B46.1:1995.

3.2.3 Practical limitations

For all microtexture scans using the Surtronic 3+, the measurement positions were not chosen at random, and chips with 'flat' regions that would not cause the instrument to go beyond its measurement range (either 0.1 mm or 0.5 mm) were deliberately selected. Finding suitably flat faces was a problem particularly for longer scans (e.g. scan length = 2.50 mm). For a true indication of microtexture, the measurement positions would be chosen at random, but this was not possible with the instrument described.

3.3 Transit NZ's Stationary Laser Profilometer (SLP)

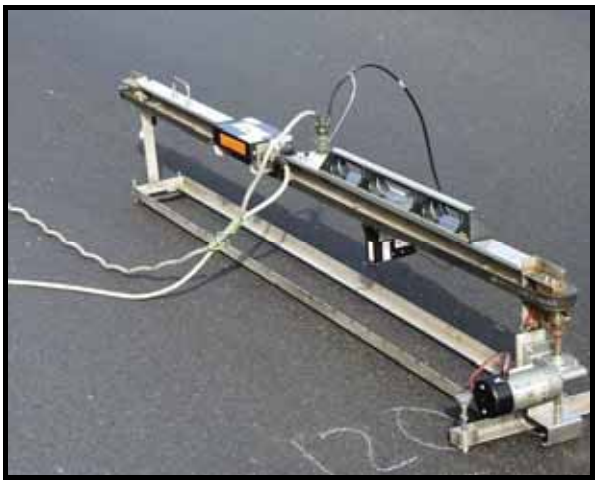

Figure 3.4 Transit NZ's SLP.

Transit NZ's SLP has been used to measure macrotexture (Figure 3.4). The SLP uses a Selcom® 32 kHz laser with a spot size of 0.5 mm and takes a profile measurement every 0.3 mm. The laser traverses along a 1.67-m track by a drive from a rubber-toothed belt. The SLP is generally used for macrotexture measurements (e.g. texture depth) and is not suitable for resolving and measuring microtexture.

Figure 3.5 shows a typical plot of a road profile measured by the SLP (using different scales). The particular example is for a grade 2 chipseal with an estimated 90% crushed faces (Cenek et al. 1998).

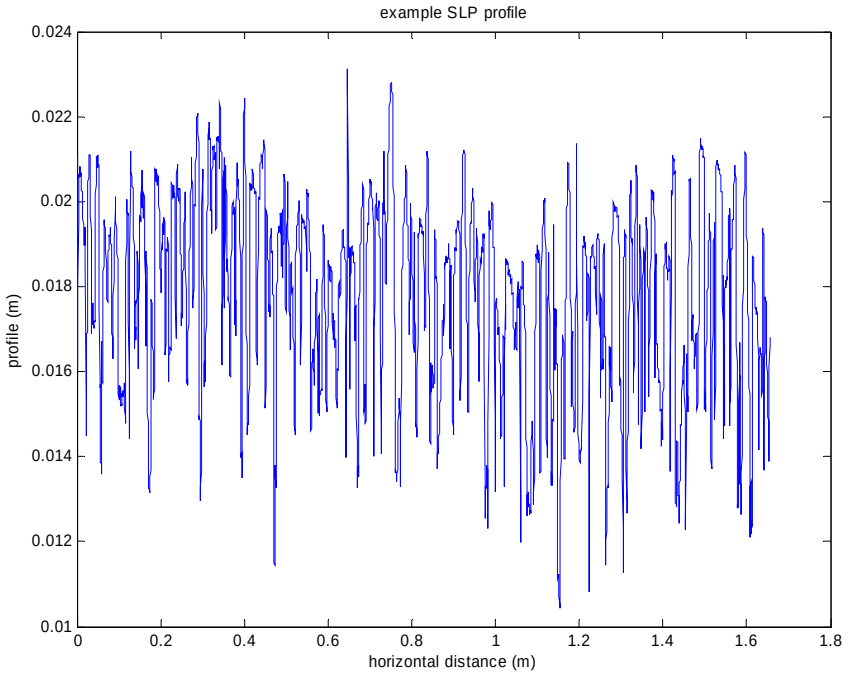

a. An SLP profile with axes not scaled equally.

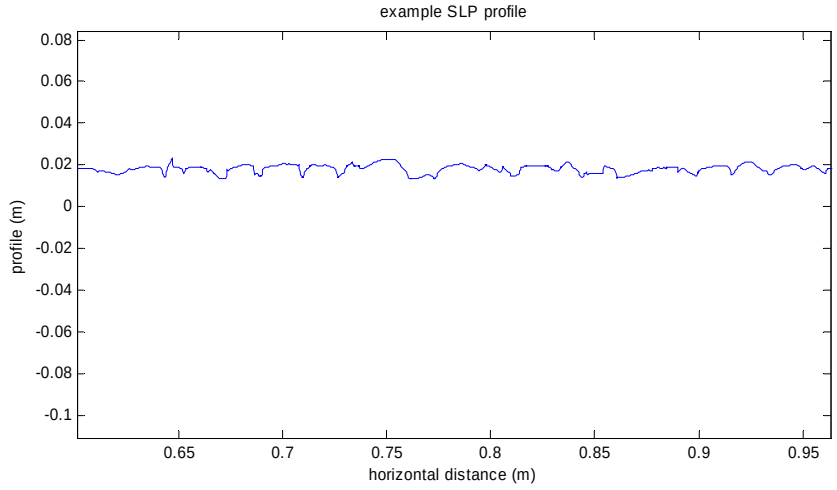

b. The same SLP profile with axes scaled equally.

Figure 3.5 Example of an SLP profile.

4. Desk-top analysis of MSSC data

Before making texture and skid resistance measurements on the pavement samples detailed later in this report, two initial desk-top investigations of the skid resistance of roads in the Hawke's Bay and Gisborne regions were completed.

For these investigations, Transit NZ's RAMM database was employed with the skid resistance data in terms of the three-year average Mean Summer SCRIM Coefficient (MSSC).

4.1 Investigation 1: Regional MSSC analysis

The purpose of this first desk-top investigation was to determine:

1. If the skid resistance of roads in the Hawke's Bay and Gisborne regions was markedly different to that for North Canterbury.
2. If the skid resistance of roads constructed with aggregate from alluvial quarries was different to roads constructed with aggregate from hard rock quarries.

Comparisons were made on the basis of the three-year average of MSSC (2000/01, 2001/02, 2002/03) for five geographic regions for straight and level sections of State Highway using single-coat grade 3 chip. The 3-year averaged MSSC is distinguished as MSSC'. Site selection details are given in Table 4.1.

Table 4.1 Site selection criteria for investigation 1.

Selection Criteria	Parameters
MSSC Surveys	2000-01, 2001-02, 2002-03
RAMM Regions	East Wanganui, Gisborne, Hawke's Bay, North Canterbury, Wellington
Seal Type	Single-coat chipseal
Chip Grade	3
Age	Greater or equal to two years old in 2000-01
Repairs	None
Unusual Features	None (adverse camber, poor drainage, bleeding, flushing)
Texture Depth	> 1.4 mm in wheelpath
Geometry	Straight (horizontal curvature >300m) and level (gradient < 5%)
TNZ T/10 Skid Site Category	4

Table 4.2 Variation of MSSC′ by region.

RAMM geographic region	Predominant quarry type	MSSC′	% of average MSSC′	Length (km)
East Wanganui	alluvial	0.486	92.6	184.41
Gisborne	alluvial	0.555	106.0	36.89
Hawke's Bay	alluvial	0.507	96.5	64.88
North Canterbury	alluvial	0.550	104.8	58.13
Wellington	hard rock	0.526	100.1	80.8

Average MSSC′ = 0.525

Statistical analysis using the software package SAS® was performed on these results but is not shown here. This analysis indicated that all of the differences in MSSC′ between the five regions are statistically significant at the 95% confidence level.

With reference to Table 4.2, observations are:

1. The MSSC′ of State Highways (SH) in the Hawke's Bay and Gisborne regions are not markedly lower than for roads in the three other regions analysed. (While the MSSC′ of Hawke's Bay is 3.5% lower than the average MSSC′ for the five regions, the MSSC′ for East Wanganui is lower again at 7.4% below the average MSSC′.)
2. The MSSC′ of SH constructed predominantly with aggregate from alluvial quarries are not markedly different from roads constructed predominantly with aggregate from hard rock quarries.

It should be emphasised that this analysis is based on data for five regions only, and the conclusions may not be true for the whole of New Zealand.

4.2 Investigation 2: Matched-pair MSSC analysis

The purpose of this second desk-top investigation was to compare the skid resistance of aggregates in Hawke's Bay with the skid resistance of the same aggregates in another region, to determine if the reportedly low level of skid resistance in Hawke's Bay could be attributed to environmental effects.

Two sets of data were used:

Data Set 1: The MSSC′ of SH in Hawke's Bay.

Data Set 2: The MSSC′ of SH chosen from regions other than Hawke's Bay using aggregate sourced from quarries common to Data Set 1.

The RAMM search indicated that aggregate from four quarries is used in more than one of the five regions of Table 4.2. As indicated by Table 4.3, these quarries are: Awatoto, Belmont, Otaki and Whitehall. Disappointingly, insufficient lane-km (Table 4.3) of

aggregate is used in the Hawke's Bay region and other regions to allow meaningful analysis, and so the matched-pair analysis was not pursued further.

Table 4.3 Lane-km of aggregate used in Hawke's Bay and other RAMM geographic regions.

Source quarry	RAMM geographic region			
	East Wanganui	Hawke's Bay	Wellington	Gisborne
Awatoto	–	0.190	–	6.120
Belmont Quarry	–	0.340	20.630	7.590
Otaki	2.000	–	5.830	–
Whitehall Quarry	–	2.240	–	6.490
Total	**2.000**	**2.770**	**26.460**	**20.200**

5. Core samples for determining skid resistance

Measurements were made on actual road surfaces to (a) determine the variation in skid resistance with HCV polishing, and (b) determine the difference in texture between aggregate from Hawke's Bay and Canterbury. In preference to on-site measurements, core samples were taken from the selected sites to allow texture measurements to be carried out in the laboratory.

5.1 Core Samples

The sites were chosen from straight and level sections of rural State Highway (SH) with single-coat chipseal surfaces. To assess the effect of HCV polishing, each site was chosen to correspond with 'low', 'medium', or 'high' levels of Heavy Commercial Vehicle (HCV) passes. Cores were taken from both the left wheelpath (trafficked) and between the wheelpaths (less trafficked). Straight and level sections of road were chosen so that the level of stress between the pavement and tyres would be similar. Sites were from two geographic regions (Hawke's Bay and Canterbury) with aggregate from either the Hastings Quarry in the Hawke's Bay, or Pound Road Quarry in Canterbury. Additional details on the site selection criteria for the core samples are listed below:

Regions:	Hawke's Bay (SH2), and Canterbury (SH1)
Quarries:	Hastings Quarry, Holcim® Aggrgeates, Hastings;
	Pound Road Quarry, Fulton Hogan Limited, Canterbury
Geometry:	Straight (horizontal curvature > 300 m)
	Level (gradient < 5%)
Grade:	3
Surface:	Single-coat chipseal
HCV Passes:	Low, medium, and high

In total, 12 core-samples were taken (i.e. 3 levels of polishing × 2 wheelpaths × 2 regions). Additional data on the cores along with images is given in Appendix 4.

Note: Roads reach an equilibrium level of polishing after 1M (million) HCV passes or 2M HCV axle passes according to research recently performed by Cenek et al. (2004). However, at the time the sites were chosen for cores, research suggested that 3M HCV passes were required to achieve an equilibrium state of polish, and so cores were selected on this basis.

5.2 Measurements of skid resistance

Two techniques were used to record the skid resistance of each core:

1. British Pendulum Tester (BPT) measurements, 1 per core.
2. MSSC from the RAMM database averaged over three years.

SCRIM measurements were used to determine skid resistance in preference to Central Laboratories GripTester for the following reasons:

1. SCRIM measurements are used by Transit NZ for SH management.
2. Variations in GripNumber can result from environmental conditions (precipitation, wind, temperature). MSSC averaged over three years reduces environmental variations.

5.2.1 BPT measurements

The British Pendulum Number (BPN) is a 'spot' measurement only, and the skid resistance measured by a BPT will vary depending on its exact location. Other surface friction test devices, such as the GripTester and SCRIM, provide friction measurements averaged over a length of pavement. Variability of BPN may thus mask the expected reduction in skid resistance with increased polishing.

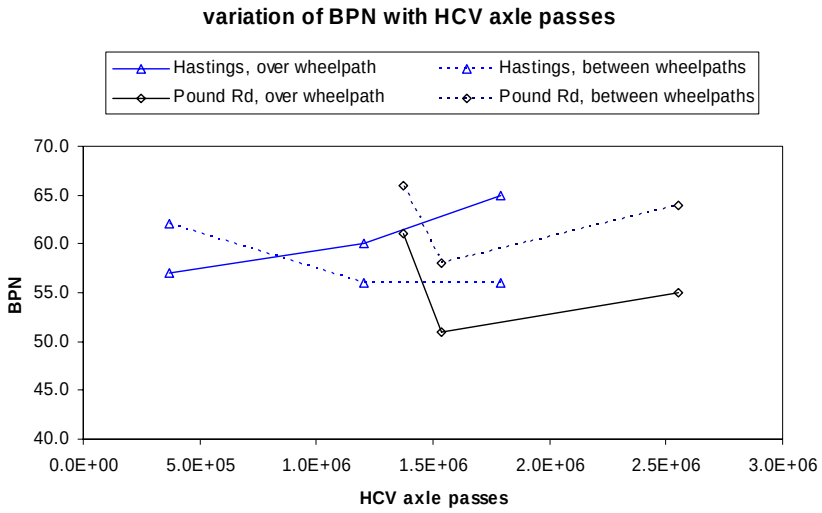

Figure 5.1 Variation of MSSC' with HCV passes.

With reference to Figure 5.1, (a) no clear reduction in BPN with HCV passes is seen, (b) the BPN of the cores taken between the wheelpaths are not markedly higher than for the cores taken over the left wheelpath, and (c) cores from one region do not show a trend of greater BPN than cores from another region.

Evidence that contamination and weather has influenced BPN on the Canterbury cores is that the cores taken in Canterbury 'over' and 'between' the wheelpaths show similar trends of BPN. In summary, no firm conclusions can be drawn from Figure 5.1.

5.2.2 MSSC measurements

For each road core, MSSC data was extracted from the RAMM database for the 10 m intervals to 100 m either side of where the core was taken. Averages were then calculated for this 210 m section and then averaged again for the years 2001-2003 inclusive.

The variation of MSSC averaged over three years is shown in Figure 5.2. Observations are:

1. The skid resistance of the cores from Canterbury (Pound Road) is greater than that of the Hastings cores.
2. MSSC' decreases with HCV passes. This observation is in accordance with expectations.

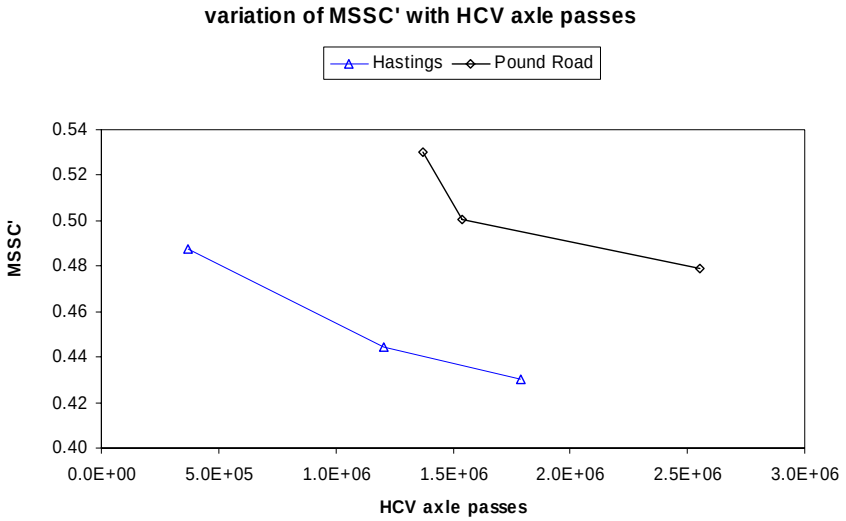

Figure 5.2 Variation of MSSC' with HCV passes.

6. The PSV test

6.1 APM polishing

6.1.1 Test method

The equipment and procedures used for polishing laboratory samples using the APM were in accordance with a standard PSV test except that:

1. One polishing run was completed instead of two.
2. The total polishing time was extended to a total of 9 hours (3 hours grit, 6 hours flour) instead of the standard 6 hours (3 hours grit, 3 hours flour) to monitor the change in microtexture over a greater period of time.
3. No corrections were made according to the PSV of the control stone.

Samples were prepared for the APM from the following quarries:

Quarries: Hastings Quarry, Holcim® Aggregates, Hastings;
Pound Road Quarry, Fulton Hogan Limited, Canterbury

Chip Grade: 4 (sieved as per PSV test procedures to give ~10 mm chip)

Sample Plates:
1. Hastings Quarry pea-gravel
2. Hastings Quarry sealing chip
3. Pound Road Quarry pea-gravel
4. Pound Road Quarry sealing chip

No. of Plates: 3 plates of each sample (i.e. 12 plates total)

PSV' tests and microtexture profile measurements were made at 0, 3, 4, 5, 6, and 9 hours of APM-polishing.

6.1.2 Results

The results in Table 6.1 show the results of PSV' test made on APM-polished samples. Note that the results shown are in terms of PSV', which is PSV obtained from a standard PSV test but only one polishing run is completed (not two), and no corrections have been made based on results for the control stone.

Table 6.1 PSV' results for APM-polished samples.

Source quarry		**Pound Road**		**Hastings Quarry**	
Chip type		seal chip	pea-gravel	seal chip	pea-gravel
Polishing	**hours**	**PSV'**			
before grit	0	77	63	72	57
3 h grit	3	68	63	63	57
1 h flour	4	56	53	54	49
2 h flour	5	53	49	50	44
3 h flour	6	53	49	49	44
6 h flour	9	51	45	47	43

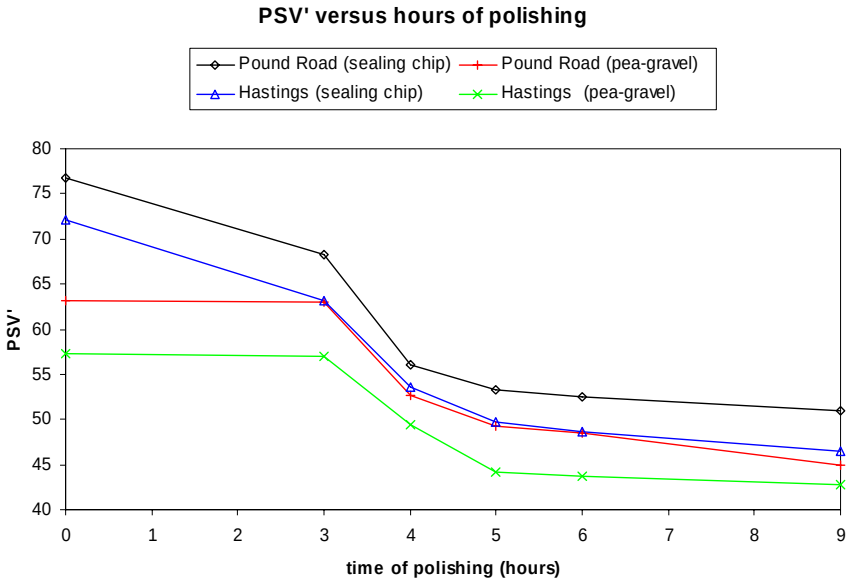

Figure 6.1 Variation of PSV' with hours of polishing.

From Figure 6.1, the following observations for the APM-polished samples can be made:

1. Pea-gravel PSV' has the same value before and at the end of emery grit polishing (0-3 hours).
2. Sealing chip PSV' decreases by approximately 9 PSV units for polishing with emery grit (0-3 hours). This reduction appears independent of the initial PSV´ of the aggregate.
3. Once the initial 3-hour period of polishing with emery grit has elapsed, the PSV' of pea-gravel from Pound Road Quarry is similar to the PSV' of sealing chip from Hastings Quarry.
4. At the completion of standard length PSV test, the PSV' of sealing chip is greater than that of pea-gravel by approximately 4.5 PSV units for aggregate from the same quarry.
5. PSV' does not decrease markedly after the standard 6-hour PSV test duration has been completed.
6. For aggregate with the same degree of crushing, the difference in PSV' for the two aggregates is similar for unpolished and APM-polished samples.
7. The PSV' increase introduced by crushing remains after APM polishing, although it is reduced in magnitude.

Note: The tolerance on PSV values has a standard deviation of 0.754; therefore small differences in PSV are not significant (EN 1097-8:1999). (The tolerance for the work described here may be greater as the standard PSV test method was not followed, see Section 3.1.1.)

6.1.3 Nominal PSV Values

For reference, Transit NZ's PSV Wall Chart entitled 'Suppliers of Surfacing Aggregate – Polished Stone Value' (September 2004) gives the PSV values for the aggregate used in these tests as in Table 6.2.

Table 6.2 Nominal polished stone values.

Quarry	PSV
Hastings Quarry, Holcim® Aggregates, Hastings	55
Pound Road Quarry, Fulton Hogan Limited, Canterbury	57

6.1.4 Supplementary PSV Tests

In an attempt to make the microtextures of chip from either of the two quarries similar, and to better understand how texture contributes to PSV', the exposed aggregate surfaces of the plates were coated in urethane and additional friction tests were carried out. Only two of the four of the plates for each sample type were tested. Measurements were made on each plate in both directions, giving a total of four PSV´ measurements per sample. The samples were not polished in addition to the 9 hours (total) recorded in Table 6.3.

Table 6.3 Supplementary PSV´ tests with urethane-coated plates after 9 hours APM polishing.

Source Quarry	Pound Road		Hastings Quarry	
Crushing	100% (sealing chip)	0% (pea-gravel)	100% (sealing chip)	0% (pea-gravel)
Number of plates	2	2	2	2
PSV'	21.25	16.5	21.5	18.8

These results are used later in Chapter 9 of this report.

6.2 Verification of APM-polishing

6.2.1 Test method

To evaluate the polishing action employed in the PSV test, direct microtexture measurements were made on both the PSV sample plates (Section 6.1.1) and the road core samples (Section 5.1) using the Surtronic 3+ (Section 3.2).

Scans were made at 'fine' and 'coarse' resolutions as it was not apparent whether a longer scan with a 'coarse' resolution would be preferable to a shorter scan at a 'fine' resolution in terms of detecting the texture that contributes to friction.

As recorded in Tables 6.4 and 6.5, the scan length at the 'coarse' resolution was 2.5 mm for the PSV plates, and 1.25 mm for the road cores. This difference in profile length was necessary as chips on the road cores did not have flat faces suitable for the longer scan length of 2.5 mm.

Each scan took between 1 minute and 5 minutes.

Table 6.4 Surtronic 3+ microtexture measurements of APM-polished samples.

Surtronic 3+ Resolution Setting	Profile Length, L (mm)	Range (μm)	Vertical Resolution (μm)	Scans per Plate	Plates Per Sample	Total Number of Scans
fine	0.25	100	0.1	6	3	432
coarse	2.5	500	0.5	6	3	432

Table 6.5 Surtronic 3+ microtexture measurements of road-polished samples.

Surtronic 3+ Resolution Setting	Profile Length, L (mm)	Range (μm)	Vertical Resolution (μm)	Scans per Core	Total Number of Scans
fine	0.25	100	0.1	10	60
coarse	1.25	500	0.5	10	60

From the measured microtexture profiles, both (a) microtexture statistics and (b) microtexture profile power spectral densities (PSDs) were calculated to enable comparison of the APM-polished and HCV (road)-polished aggregate to be made.

6.2.2 Results

A summary of results is given in Appendices 7, 9 and 13. These results indicate that:

1. the relationship between polishing and microtexture measured by the Surtronic 3+ is not sufficiently strong to be useable; and
2. direct microtexture profile measurement is only suitable for differentiating between aggregates.

An example of a microtexture profile PSD is shown in Figure 6.2. It shows that microtexture profiles are similar whether polished by the APM or by HCV tyres. This may be a function of the measurement technique or processing, or it may indicate that the microtexture profiles are similar when APM-polished or HCV (road)-polished.

Possible reasons for the lack of clear difference in aggregate microtextures shown in Figure 6.2 are:

1. An insufficient number of microtexture profile scans. (While performing a greater number of scans could be expected to reduce experimental fluctuations, this approach would be time-consuming and therefore uneconomic.)
2. Surface irregularities with a radius of less than 5 μm may provide a major contribution to skid resistance, and these irregularities were not adequately measured by the stylus, which in this case had a tip radius of 5 μm.
3. The aggregate surface may be damaged and altered during the measurement process. (This is judged unlikely, as the force between the stylus and surface to be tested is negligible.)

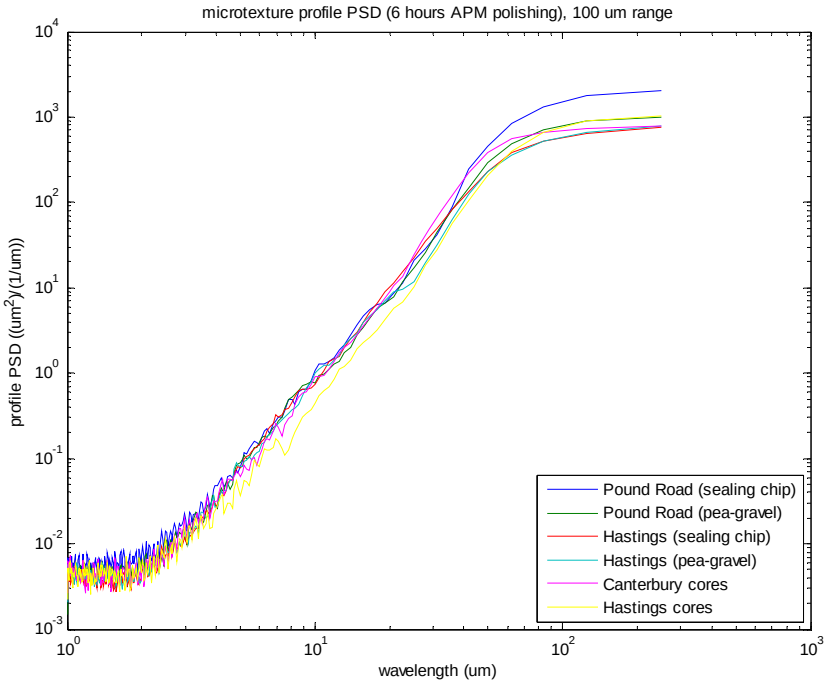

Figure 6.2 Comparison of APM-polished and HCV (road)-polished aggregates.

Note: The core microtextures are of the core taken over the left wheelpath for a 'high' level of HCV passes.

4. The stylus may tend to 'wander' to avoid larger aggregate irregularities and so the scanned profiles may not be representative of the actual aggregate surfaces. (The stylus is inherently flexible in the lateral direction because of its design.)
5. Flat areas of chips were selected for scanning to prevent the machine going out of range, rather than the positions of scans being chosen at random.

On the basis of these comments, an instrument such as the Surtronic 3+ is not recommended for use to assess the microtexture of aggregates. It is not therefore possible to accurately compare polishing of the APM with polishing by HCV tyres by this method.

7. Macrotexture polishing

7.1 Theoretical enveloping analysis

Figures 7.1 and 7.2 show predicted tyre–chipseal contact regions and contact pressures based on an enveloping analysis method detailed by Fong (1988). This analysis method uses three items of information:

1. The texture profile of the pavement surface.
2. The inflation pressure of the tyre (90 psi).
3. The tread rubber stiffness of the tyre (5 MPa).

The values used for this analysis were chosen to be typical of a truck tyre.

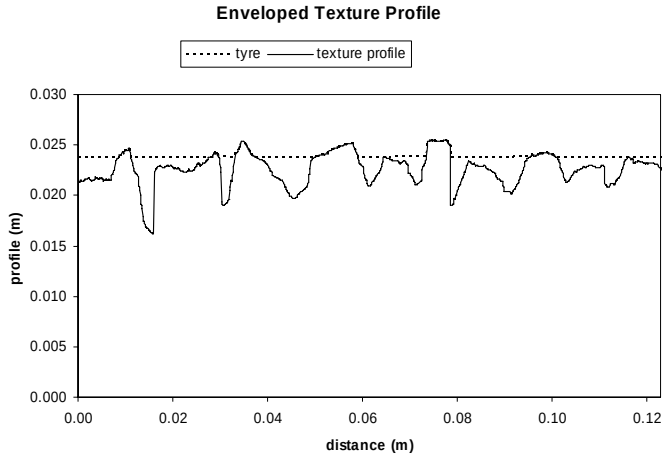

Figure 7.1 Predicted contact profile.

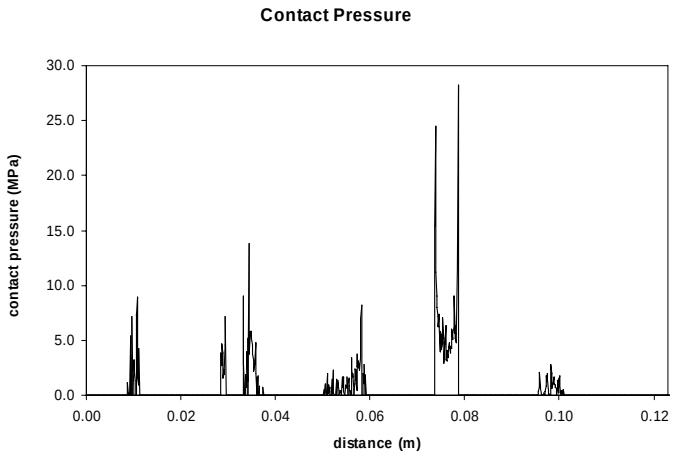

Figure 7.2 Predicted contact pressure.

Observations were:

1. The tyre makes contact only with the asperity tips of a chipseal surface.
2. Peaks in contact pressure coincide with 'sharp' asperities.

Given these observations, a chipseal surface constructed using a coarse chip (e.g. grade 2 or 3) will, probably, have fewer points of contact and therefore higher contact pressures with the tyre than a surface using a finer chip (e.g. grade 4 or 5). A surface using a coarse chip would therefore be expected to polish more rapidly than a surface using a finer chip. Polishing would affect not only the microtexture, but would also tend to round the sharp edges that might serve to contribute to hysteretic friction. Conceivably the two mechanisms by which skid resistance would reduce with increasing HCV passes are microtexture polishing and macrotexture polishing.

7.2 SLP analysis

To provide quantitative information on the effect of chipseal profile changes due to polishing, Transit NZ's Stationary Laser Profiler (SLP) was used to measure the profiles of the road cores described in Section 5.1. Eighty scans were made on each core at a spacing of 1 mm. Each scan was 100 mm in length. Three methods of analysis were undertaken, as described in Table 7.1.

Table 7.1 Analysis methods for SLP measurements.

Analysis method	Description
1. Statistics of texture profile	The statistics as summarised by Cenek et al. (2004)
2. Power Spectral Density (PSD) of texture profile	The average of the PSD for each core
3. Texture and enveloping statistics of enveloped texture profile	The statistics of the enveloped profile. Statistics considered were: (i) Mean wavelength (ii) Mean contact pressure (iii) Mean average absolute slope (iv) Average amplitude (v) Mean peak contact pressure (vi) Mean roughness average

These analysis methods failed to differentiate cores on the basis of polishing. This was judged to be caused by variations in:

1. Percent crushing;
2. Chip packing;
3. Chip shape.

It is thought that these variations tended to be the dominant influences on the profiles measured by the SLP, leaving the effect of changes in texture caused by polishing hard to distinguish.

8. GripTester and BPT friction measurements

The GripTester and BPT were used to directly determine skid resistance variations with (a) source quarry, and (b) percent crushing.

Measurements were made in the laboratory using 'artificial' road surfaces rather than actual road surfaces. This decision was made for the following reasons:

1. Skid resistance on actual road surfaces is a function not only of percent of aggregate crushing, but also environmental conditions, source quarry, trafficking, and road geometry. In the laboratory, these variables can be made constant or eliminated.
2. An insufficient number of road sites are available that have low levels of crushing. (Most chipseal surfaces use aggregate that has >70% crushed faces.)
3. The percent crushed faces is difficult to accurately determine by visually examining a chipseal surface.
4. The percentage of crushed faces on a particular site is not possible to assess properly without visually inspecting its surface. This would make choosing sites both time-consuming and expensive.

8.1 Test surfaces

The test surfaces were constructed by bonding aggregate from Pound Road and Hastings Quarry to wooden bases for a range of percent crushing values. Aggregate 'rolling', normally achieved by the action of traffic, was carried out in the laboratory by using a flat wooden block to re-orient the aggregate chips with their aggregate least dimensions (ALD) predominantly vertical. Data for the test plates are shown in Table 8.1, and digital photographs in Appendix 2. In total, 11 plates were manufactured.

Table 8.1 Test plate data.

Aggregate source	Supplied chip grade	Sieve size (pass)	Sieve size (held)	Binder	Base	% crushing
Pound Road	4	13.2	8.0	FOSROC™ epoxy	500×185×10 mm plywood	0, 50, 70, 80, 90, 100
Hastings Quarry	4	13.2	8.0	FOSROC™ epoxy	500×150×10 mm plywood	0, 50, 80, 90, 100

Note: The width of the plates for aggregate from Pound Road was 185 mm, and the width of plates for the Hastings Quarry aggregate was 150 mm. This difference in width is not expected to influence the results as the GripTester was positioned so that it would pass over the centre of each plate (test wheel width = 100 mm).

The following differences were noted during sieving (before the test plates were manufactured), and also visually after the test plates had been tested:

1. The pea-gravel from Hastings Quarry was smaller than the pea-gravel from Pound Road Quarry.

2. The sealing chip from Hastings Quarry was smaller than sealing chip from Pound Road Quarry.
3. The pea-gravel from Hastings quarry had a less regular shape than pea-gravel from Pound Road Quarry.

On the basis of item 3, the hysteretic component of friction would be expected to be greater on plates made from Hastings Quarry chip than on plates made from Pound Road Quarry chip.

8.2 GripTester measurements

8.2.1 GripTester slip

GripTester measurements were carried out on a dry smooth concrete floor (GN = 0.56) in the laboratory. The treaded drive-wheels of the GripTester rolled on the concrete floor, while the centre measurement wheel rolled on the test surfaces.

GripTester numbers might thus be atypical as the driven and test wheels would normally roll on the same surface, possibly introducing some variability in the degree of slip (normally 15%) depending on the difference between plate and floor friction. (This would be due to the front treaded pair of wheels to slip/skid rather than roll on the concrete floor.)

Consequently, the 15% degree of slip cannot be assumed to be constant and the GripNumber (GN) is reported as being a 'modified' GripNumber (GN'). However, in practice, the variation in slip is expected to be negligible as:

- Slip of the treaded wheels on the concrete floor was not apparent to the GripTester operator during testing.
- The treaded front wheels of the GripTester take the bulk of the weight of the GripTester (31.5 kg per wheel), and would therefore be less likely to slip than the measurement wheel which takes less of the load (22 kg). Simple theory comparing the force required to induce slip on the wheels indicates that the treaded wheels will not slip/skid provided that:

$$2 \times M_f \times \mu_c \geq 1 \times M_m \times \mu_p \qquad \text{Equation 8.1}$$

where:

M_f = Load on each treaded front wheel = 31.5 kg per wheel

μ_c = GN of concrete floor = 0.56

M_m = Load on measurement wheel = 22 kg

μ_p = Maximum GN' of test plates = 0.99 (test 2, 100% crushed chip)

Substituting these values in Equation 8.1 gives:

$$\mu_c \geq 0.35 \times \mu_p. \qquad \text{Equation 8.2}$$

Equation 8.2 holds true for all the tests described here, and slip of the front wheels would not be expected to occur.

8.2.2 GN' test procedure

The test plates were tested simultaneously by positioning them lengthwise as shown in Figure 8.1.

Figure 8.1 GripTester measurements (operator's view).

The GripTester was used in 'calibrate' mode to give a skid number reading every 40 mm (i.e. 12 skid number readings per plate). To reduce any influence of variations in skid resistance of (a) the concrete floor, or (b) plate direction, 22 runs were completed for each test. Details of the runs are below and, in total, each test consisted of 264 friction readings per plate (i.e. 12×22).

Table 8.2 Test run data.

Runs	Plate orientation	Plate indexing
1-11	Forward	plates indexed[1] 1 position for each run
12-22	Reverse	plates indexed[1] 1 position for each run

[1] Plates indexed = plate order changed by moving the last plate to first plate position, and moving the remaining plates up 1 position (i.e. run 1 plate order = 1-11; run 2 plate order = 2-11, 1; run 3 plate order = 3-11, 1-2; etc.).

The GripTester tended to 'bounce' at the interface between one plate and the next. To provide a smoother transition between plates, wooden inserts were placed between the test plates. In spite of this, 'bounce' was still evident both to the GripTester operator, and in the results. An example trace is given in Appendix 10.

While the predicted GN' might be a function of how a particular plate mates with its neighbours, this effect has been minimised by (a) reversing the orientation of the plates, and (b) indexing the plates (Table 8.2).

Importantly, errors in the measured trend of GN' with the percentage of crushed chip do not show strong systematic trends due to GripTester 'bounce'.

All data processing and analysis was carried out using Matlab®, release 14.

Figure 8.2 Test plates showing wooden-inserts to reduce GripTester 'bounce'.

8.2.3 GN' measurements

Table 8.3 GripTester measurements.

Test Number	Surface	Number of Varnish/ Urethane Coats	Wet/Dry
1	New and unpolished	none	Dry
2	New and unpolished	none	Wet
3	Varnish coated	1	Dry
4	Urethane-coated	1	Wet
5	Urethane-coated	3	Wet

To estimate the contribution of hysteretic friction, varnish/urethane-coatings were applied to the plates before testing (tests numbers 3-5). The intention was to 'mask' the microtexture, so that any difference in the GripNumber of the plates would be related to their shape and size only (a function of the sieving process and crushing process), and not to their microtexture.

Notes:

- Water was applied to the plates from a hand-sprayer of the type typically used by gardeners to apply spray for home use. For the first few runs, water was applied at the completion of each run, but for subsequent runs, water was applied only after every second run. Water was applied to the test plates only, and not to the surrounding surface of the concrete floor.
- For test number 5, three coats of urethane were sprayed onto the plates. The thickness of the coating was insufficient to alter the macrotexture, and was estimated to mask only the shorter microtexture wavelengths. This coating did not wear through during testing.

8.2.4 GN' results

Figure 8.3, which is based on the data in Table 8.4, shows the results of tests 2 and 5. It is evident that for the uncoated chips (test 2):

- The GN' of aggregate from both Pound Road and Hastings Quarries increases linearly with the percentage of crushed chips by approximately 0.27 GN' units. (The GN' is 0.7 for 0% crushed chips, and 0.97 for 100% crushed chips.)
- Aggregate from Pound Road shows evidence that it has a slightly greater GN' than aggregate from Hastings Quarry by approximately 0.02 GN' units. This is in agreement with the reported PSV results for these two sources (Table 6.2).
- Plates made from Pound Road chips when 90% crushed have a similar GN' to plates made from Hastings Quarry chips when 100% crushed.

It is evident that for the urethane-coated chips (test 5):

- When coated with urethane, the GN' increases linearly with the percentage of crushed chips.
- When coated with urethane, the GN' of aggregate from both Pound Road and Hastings Quarries increases only slightly with percent crushing. (The increase is approximately 0.04 GN' units for test 5 compared to 0.27 GN' for test 2.)
- When coated with urethane, aggregate from Hastings Quarry has a slightly greater GN' than aggregate from Pound Road by approximately 0.03 GN' units. This is a reversal of their natural ranking, i.e. aggregate from Pound Road has a higher PSV than aggregate from Hastings Quarry (see Table 6.2).
- The GN' of urethane-coated chips is very low compared with uncoated chips.

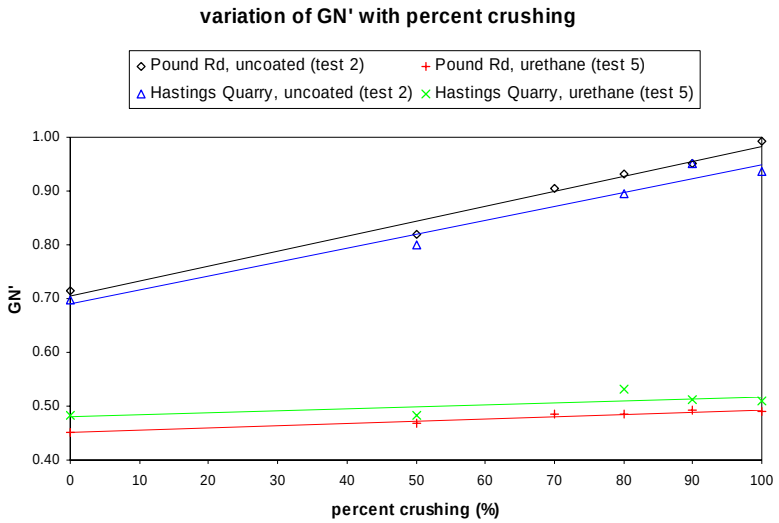

Figure 8.3 Variation of GN' with percent crushing.

Table 8.4 BPN tests on urethane-coated plates.

Aggregate source	Surface coating	Test number (Table 8.3)	Percent crushing (%)	GN'
Pound Road	New and uncoated	2	0	0.72
		2	50	0.82
		2	70	0.90
		2	80	0.93
		2	90	0.95
		2	100	0.99
	Urethane-coated	5	0	0.45
		5	50	0.47
		5	70	0.49
		5	80	0.49
		5	90	0.49
		5	100	0.49
Hastings Quarry	New and uncoated	2	0	0.70
		2	50	0.80
		2	80	0.90
		2	90	0.95
		2	100	0.94
	Urethane-coated	5	0	0.48
		5	50	0.48
		5	80	0.53
		5	90	0.51
		5	100	0.51

Note: Only the results of tests 2 and 5 are shown in this report, as the other tests are not useful in terms of determining the increase in surface friction with percent crushing.

8.3 BPN measurements

To supplement the GripTester skid resistance measurements described in the foregoing text, BPT skid resistance tests were used. These additional tests were undertaken primarily to confirm or negate the GripTester data which showed only a small increase in skid resistance for urethane-coated aggregate with percent crushing (e.g. 0.04 increase in GN' from 0 to 100% crushed chips).

8.3.1 BPN tests on urethane-coated plates

BPN measurements were undertaken on the urethane-coated plates used for GripTester measurements (i.e. test 5, Table 8.3). Results are recorded in Table 8.5 and shown graphically in Figure 8.4.

Six BPN measurement positions were used for each plate (Table 8.5), three for the plate in one direction, and three for the plate in the opposite direction. The three measurements were made at the left-hand side, middle, and right–hand side of each plate.

Table 8.5 BPN tests on urethane-coated chipseal plates.

Aggregate source	Number of measurement positions	Percent crushing (%)	BPN (average, 6 positions)	BPN (standard deviation, 6 positions)
Pound Road	6	0	23.8	2.2
		50	26.3	2.2
		70	29.2	2.2
		80	32.0	2.4
		90	31.7	2.7
		100	31.7	2.1
Hastings Quarry	6	0	26.8	2.5
		50	33.3	4.4
		80	35.2	4.1
		90	39.8	5.6
		100	42.7	4.3

In Figure 8.4, the straight lines shown in the figure are lines of best fit determined by the least squares technique. Notes are:

- BPN increases linearly with the percentage of crushed chips.
- The increase in BPN in going from a surface with 0% crushed chip to a surface with 100% crushed chip has an average of approximately 12 BPN units (9 BPN for Pound Road, and 15 BPN for Hastings Quarry).
- The BPN of chip from Pound Road is less than the chip from Hastings Quarry. This is a reversal of their natural ranking, i.e. aggregate from Pound Road has a higher PSV' than aggregate from Hastings Quarry (see Table 6.2).

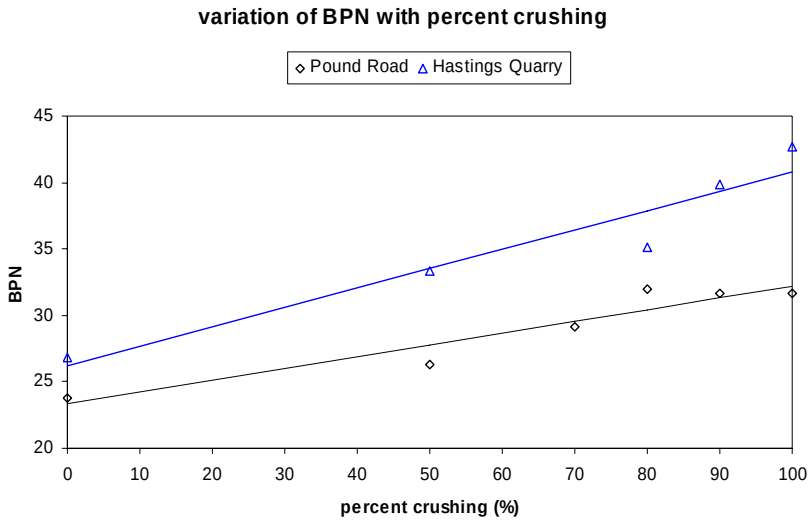

Figure 8.4 Variation of BPN with percent crushing, urethane-coated plates (R^2 = 0.907 (Pound Road), R^2 = 0.923 (Hastings Quarry)).

8.3.2 BPN tests on uncoated plates

As well as the BPN tests on the urethane-coated plates described in the previous section, additional tests were carried out on uncoated plates containing new and unpolished chips (Table 8.6).

Table 8.6 BPN tests on new and uncoated chipseal plates (grades 2, 3 and 4).

Grade	Percent crushing (%)	Number of measurement positions	Average BPN	Standard deviation
2	0	2	70	1.4
	25	3	73	13.2
	50	2	79	8.5
	75	1	84	n/a
	100	0	n/a	n/a
3	0	3	70	5.0
	25	3	78	2.0
	50	3	80	6.1
	75	3	79	7.2
	100	3	83	2.1
4	0	9	70	3.9
	25	9	76	9.9
	50	9	79	4.3
	75	9	87	3.9
	100	9	89	8.9

Notes (to Table 8.6):

1. For the reasons outlined in Section 2.5.1, the number of measurement positions ranged between 0 and 3 for the plates with the largest chips (i.e. grade 2). (While 3 measurements were intended to be undertaken on the grade 2 plates, it became apparent during the BPN measurements that the plates were too small to allow a sufficient number of suitable measurement positions.)
2. To reduce the effect of experimental variation, 6 additional measurements were carried out on the grade 4 plates, giving a total of 9 measurement positions.

The plates were constructed using aggregate from the Pound Road Quarry glued to custom wood bases (300 mm × 150 mm × 18 mm). In total, 15 plates were prepared (Grades = 2, 3, 4; percent crushed chips = 0, 25, 50, 75, 100). FOSROC™ epoxy was used as the binder.

While an effort was made to arrange the chips so that they would be typical of an actual road surface, retrospective visual inspection showed that the packing of the chip was 'looser' than would be normal. Because of this, the trends of BPN with chip grade and percent crushing will be valid, but the absolute numbers might not be typical of what would be found on the road. Photos of these plates are shown in Appendix 1.

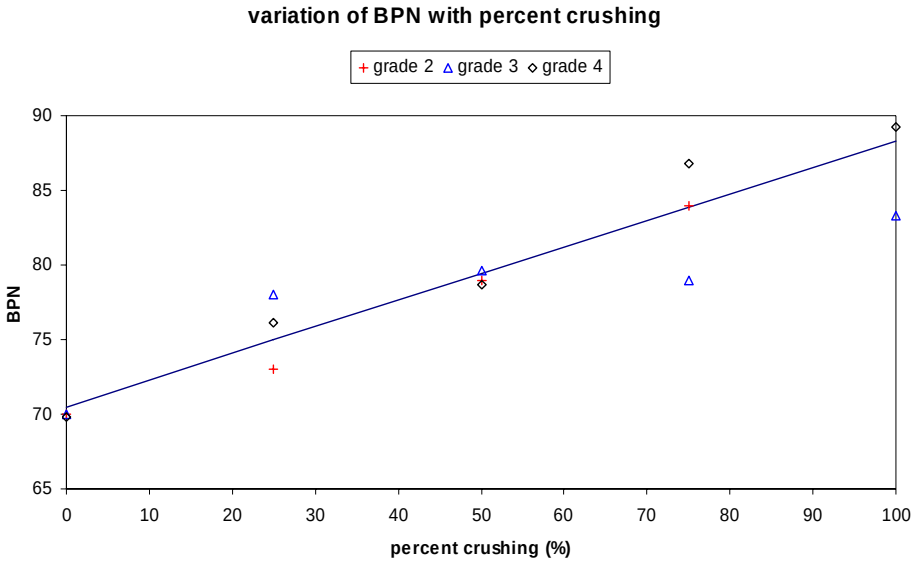

Figure 8.5 Variation of BPN with percent crushing for new uncoated chip (R^2 = 0.997).

Observations from Figure 8.5 are:

- BPN for new uncoated chip increases linearly with percent crushing.
- The increase in BPN from a surface with 0% crushed chip to a surface with 100% crushed chip is approximately 18 BPN units. (This compares with an average increase of 12 BPN units for urethane-coated chips.)
- No clear difference is evident between the BPN of plates made from grade 2, grade 3, or grade 4 chip.

8.4 Discussion of GripTester and BPN test results

1. For urethane-coated plates, the GripTester and BPT show different trends with an increase in the percentage of crushed chips. For the GripTester, there is little increase in GN' with percent crushing (0.04 GN' units, Figure 8.3), whereas the increase in BPN is large (12 BPN units, Figure 8.4).
2. For urethane-coated plates, the BPN of plates made from Hastings Quarry aggregate is greater than that of the plates made from Pound Road aggregate. Since the PSV' results (Figure 6.1) show that the PSV' at 0 hours polishing is greater for aggregate from Pound Road than for aggregate from Hastings Quarry, conclusions that can be made are that:
   - 3 coats of urethane effectively make the microtexture of the aggregates the same,
   - the shape of chip from Hastings Quarry produces more hysteretic friction than chip from Pound Road. (The shape of pea-gravel is likely to be a function of natural processes, while the shape of sealing chip may be related to (a) the method of crushing (e.g. Barmac[2] or Cone), (b) the sieving/sorting method, and/or (c) the source stock (hardness, shape, size, presence of softer seams of material, etc.).
3. For uncoated plates, there is no clear relationship between chip grade and BPN.

8.5 Comparison of GN' and BPN measurements

Differences between trends of skid resistance change with percent crushing measured by the GripTester and BPN on the urethane-coated plates may result from the relatively slow slip speed of the GripTester compared to the BPT (Chapter 2). Alternatively, the GripTester measurements may be erroneous due to:

1. GripTester wheel slip (Section 8.2.1);
2. GripTester bounce (Section 8.2.2).

Irrespective of the cause of the difference in GripTester and BPN skid resistance trends, this needs to be investigated further.

As the BPN measurements were carried out in accordance with standard procedures and are not subject to the uncertainties with the GripTester measurements, BPN measurements are used for model development in the following Chapter 9.

[2] Barmac, Cone – types of aggregate crushers.

9. Relating skid resistance to percent crushing

In this chapter, a model is developed to estimate the friction related to the percentage of crushed chips. This estimate is limited as it:

1. uses data on aggregates from only two source quarries;
2. relies only on data from laboratory-prepared plates rather than data from in-field chipseal surfaces;
3. uses data from APM-polished aggregate rather than HCV-polished aggregate.

While the model may not give numbers that are accurate in absolute terms, the trends obtained are useful for better understanding how the percentage of crushing increases skid resistance. The skid resistance measurements predicted by the model are in terms of BPN (Section 8.3).

9.1 Model construction

9.1.1 Effect of chip grade on BPN

With reference to Figure 8.5, there is no clear relationship between chip grade and BPN. For this reason, chip grade is not incorporated in the model to predict BPN.

9.1.2 Components of friction

As discussed in Section 2.1, there are two main components of friction:

1. Adhesion
2. Hysteresis

Expressed as an equation, this is:

$$F = F_a + F_h \qquad \text{Equation 9.1}$$

With this premise as a basis, a simple equation corresponding to the measured BPN results (Table 8.5) has been developed (Equation 9.2).

$$BPN = \mu_a + (\mu_c + \mu_v) \qquad \text{Equation 9.2}$$

This equation has three components, which are explained in Table 9.1.

Table 9.1 Components of Equation 9.2.

BPN Component	Symbol	Explanation	Contribution
Adhesion friction	μ_a	The adhesion component of BPN: this component increases linearly with the percentage of crushed chips	Microtexture
Constant hysteretic friction	μ_c	The constant hysteretic component of BPN corresponding to uncrushed chip (i.e. 0% crushing)	Shape of pea-gravel
Variable hysteretic friction	μ_v	The variable hysteretic component of BPN increase due to using crushed chip: it increases linearly with the percentage of crushed chip and relates to 'angular' chips rather than 'round' chips	Shape of sealing chip

By noting that BPN increases linearly with percent crushing (e.g. Figure 8.4), Equation 9.2 can be written as:

$$BPN = a([1 - P]PSV_0 + P\,PSV_{100}) + (\mu_c + P\,\Delta\mu_v) \qquad \text{Equation 9.3}$$

where:

a	=	a constant converting PSV' into the adhesion component of BPN
P	=	the proportion of crushed chips (i.e. the percentage of crushed chips divided by 100)
PSV_0	=	PSV' for 0% crushed chips
PSV_{100}	=	PSV' for 100% crushed chips
μ_c	=	the constant hysteretic component of BPN for 0% crushed chips
$\Delta\mu_v$	=	the coefficient for the variable hysteretic component of BPN

While Equation 9.3 might seem more complicated than necessary, given that BPN increases linearly with percent crushing, both the 'slope' and 'intercept' depend upon PSV_0, so the term '$(1 - p)PSV_0$' must be included.

9.1.2.1 Adhesion friction

Equation 9.3 assumes that the PSV friction test measures purely adhesion friction and not the contribution of hysteretic friction. In fact, PSV friction measurements will contain a contribution from both adhesion friction and hysteretic friction, but this is not of concern as both the adhesion component (μ_a) and the hysteretic component ($\mu_c + \mu_v$) in Equation 9.3 increase linearly with percent crushing. Therefore, there will be no error in assigning PSV' as resulting purely from adhesion friction rather than adhesion and hysteretic friction.

9.1.2.2 Constant hysteretic friction

The constant hysteretic component of friction (μ_c) is the hysteretic friction associated with 0% crushed chips. Its magnitude will depend solely on the hysteretic component of friction for pea-gravel. It will vary depending on (a) chip shape and (b) chip packing.

9.1.2.3 Variable hysteretic friction

The variable component of hysteretic friction (μ_v) is the hysteretic friction related to chip crushing. Its magnitude will vary depending on (a) shape of 0% crushed chip, (b) shape of 100% crushed chip, and (c) chip packing.

9.2 Model calibration

Table 9.2 Data for calculation of the constants in Table 9.3.

Data source	Description
Table 6.1	PSV′ of uncoated chip
Table 6.3	PSV′ of urethane-coated chip at 9 hours (total) of APM polishing
Table 8.5	BPN of urethane-coated chipseal plates
Table 8.6	BPN of new and uncoated chipseal plates

The model of Equation 9.3 has been calibrated and validated for three sets of experimental BPN data with constants being determined either from (a) experimental PSV' values (for constant 'a', PSV_0 and PSV_{100}), or (b) directly from experimental BPN measurements (for μ_c and $\Delta\mu_v$). The source data used for this are summarised in Table 9.2 and calculated constants are shown in Table 9.3.

Table 9.3 Constants for Equation 9.3.

Source quarry		Pound Road	Pound Road	Hastings
Surface		new, unpolished	urethane-coated	urethane-coated
Parameter	a	1.03	1.03	1.03
	PSV_0	63.1	16.5	18.8
	PSV_{100}	76.8	21.25	21.5
	μ_c	5.77	5.77	6.93
	$\Delta\mu_v$	4.88	4.88	11.7

The predictions from Equation 9.3 and experimental data are compared in Figure 9.1 for:

1. New and unpolished aggregate from Pound Road
2. Urethane-coated aggregate from Pound Road
3. Urethane-coated aggregate from Hastings Quarry

The straight lines on the graph correspond to the predictions of Equation 9.3, and the markers to the experimentally measured values.

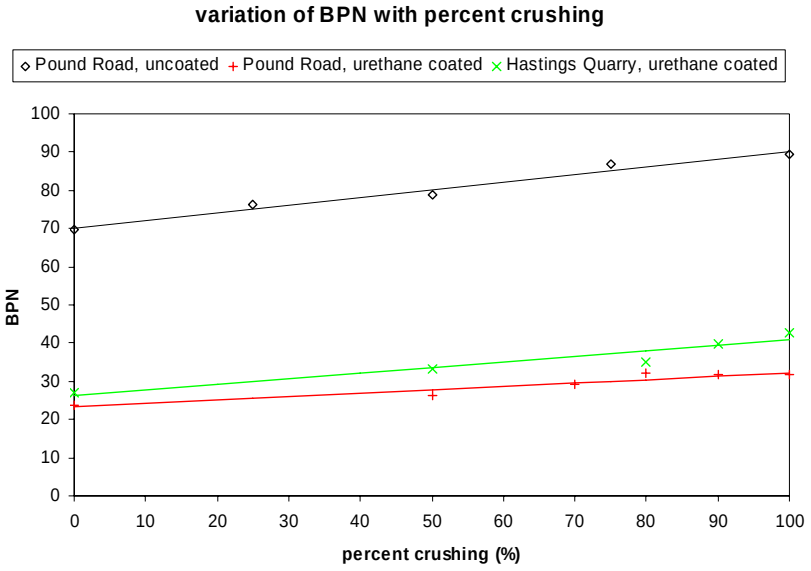

Figure 9.1 Variation of BPN: actual and predicted (Equation 9.3).

In lieu of estimating the statistical variation of the constants given in Table 9.3, predictions of Equation 9.3 have been compared directly with the experimental source data. It is evident that there is good agreement. Specifically, correlations are:

1. Pound Road, urethane-coated: R^2 = 0.907
2. Pound Road, uncoated: R^2 = 0.973
3. Hastings Quarry, urethane-coated: R^2 = 0.923

The model is thus a good representation of the experimental source data.

Note that Table 9.3 and Figure 9.1 do not show results for uncoated aggregate from Hastings Quarry, because the plates made of chip from Hastings Quarry were unintentionally coated in urethane before BPN measurements were made. Insufficient research funds were available to manufacture and test another set of uncoated plates.

9.3 Components of BPN friction

Using Equation 9.3 with the constants for new and unpolished Pound Road aggregate (Table 9.3), the components of BPN have been calculated and are shown in Figure 9.2. Observations are:

3. The adhesion component of friction (μ_a) contributes between 88% and 92% of the total friction.
4. The constant component of hysteretic friction (μ_c) contributes between 6% and 8% of the total friction.
5. The variable component of hysteretic friction (μ_v) contributes between 0% and 5% of the total friction.

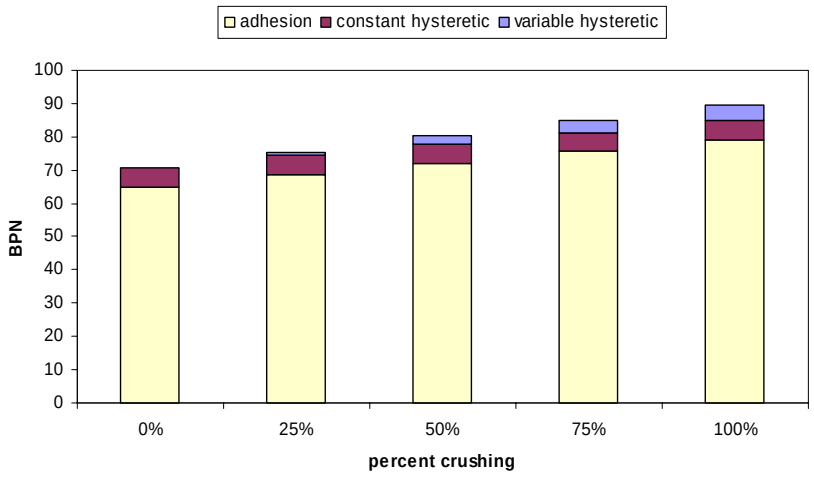

Figure 9.2 The components of BPN friction (Pound Road aggregate, new and unpolished).

In other words, for new and unpolished aggregate from Pound Road, the increase in skid resistance from 0% to 100% crushed chips is 19 BPN (increase of 27%). This increase in skid resistance has two contributions:

1. Crushed faces have a greater PSV than uncrushed faces (approximately 90% of the increase). This is related to adhesion friction (Section 2.1.1).
2. The shape of crushed chips is more 'angular' than that of uncrushed chips (approximately 10% of the increase). This is related to hysteretic friction (Section 2.1.2).

On the basis of this, most of the increase in skid resistance with percent crushing for new and unpolished aggregate is related to (a) the increased PSV of crushed faces (adhesion friction) rather than to (b) the increased angularity of crushed chips (hysteretic friction).

9.4 Model predictions for on-road terminally-polished chip

Two assumptions have been made to estimate the BPN of on-road terminally-polished chipseal surfaces from Equation 9.3. These assumptions are:

1. The PSV friction test can be used as a surrogate measure of skid resistance for aggregates in their terminal state of polish. Inherent in this assumption is that the polishing action of the APM is similar to the polishing action of HCV tyres.
2. The aggregate is polished to the extent that there is no increase in hysteretic friction due to crushing (i.e. $\mu_v = 0$). This assumption would appear reasonable, as close visual inspection of highly polished cores (e.g. Figures A4.3 and A4.9, Appendix 4) show that the asperity tips are highly polished and are indistinguishable whether originally crushed or not. This is to be expected as the tyre contacts only the asperity tips (e.g. Figure 7.1).

With these assumptions, the constants for Equation 9.3 were obtained as summarised in Section 9.2. The actual values used are recorded in Table 9.4.

While validating these predictions of BPN with actual measurements on polished road surfaces would be preferable rather than using Equation 9.3, the absence of polished roads constructed with a range of proportions of crushed chip has made this impossible.

Table 9.4 Values to use in Equation 9.3 for on-road terminally-polished chipseal surfaces.

Source Quarry		**Pound Road**	**Pound Road**	**Hastings**	**Hastings**
Surface		new, unpolished	terminally-polished	new, unpolished	terminally-polished
Measured/ Predicted		measured	predicted	predicted	predicted
Parameter	A	1.03	1.03	1.03	1.03
	PSV_0	63.1	48.6	57.3	43. 7
	PSV_{100}	76.8	52.6	72.1	48. 7
	μ_c	5.77	5.77	6.93	6.93
	$\Delta\mu_v$	4.88	0	11.7	0

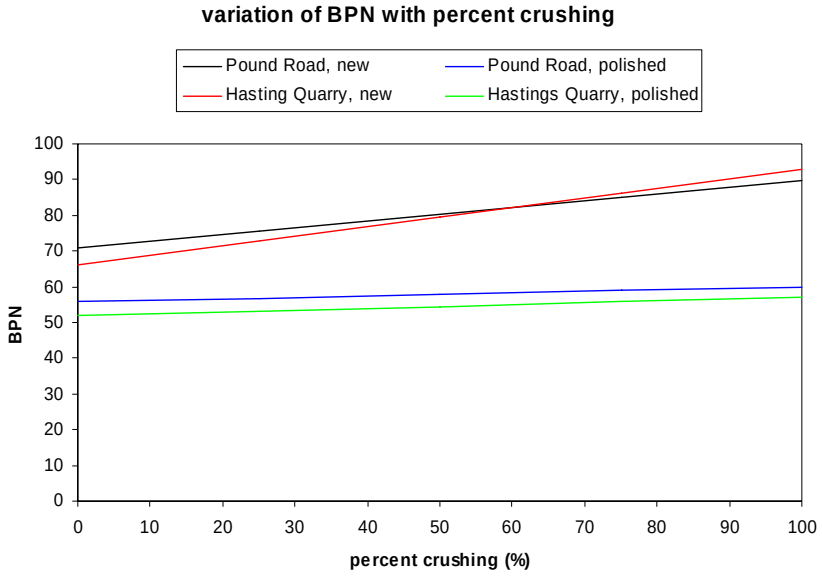

Figure 9.3 Predicted variation of BPN: new and on-road terminally-polished aggregate.

Using the constants given in Table 9.4, Figure 9.3 compares the BPN of on-road terminally-polished and new chipseal surfaces as a function of percentage crushing. As new aggregate polishes, Figure 9.3 shows that the beneficial effect of crushing becomes less marked. This is because:

1. The microtexture of crushed faces when polished becomes more similar to the microtexture of uncrushed faces (e.g. Figure 6.1).
2. Asperities that contact the tyre become 'rounded' with HCV polishing whether the chips were initially crushed or not. (In other words, while the microtexture of a chipseal reaches an equilibrium level of polish, this is not true of macrotexture. The more HCV passes experienced by a chipseal, the more similar the macrotexture profile of uncrushed and crushed chipseals will be.)

9.5 SFC predictions from BPN

As SFC (Sideways Force Coefficient) is measured by the SCRIM in annual SH surveys commissioned by Transit NZ, a graph estimating the expected variation of SFC with percent crushing is shown in Figure 9.4. The graph uses Equation 9.3 with the constants in Table 9.4 to first calculate BPN (Figure 9.3). The BPN-to-SFC conversion equation derived by the PIARC Technical Committee C1 (PIARC 1995) is then used to convert BPN predictions into SFC predictions. Details of this conversion can be found in Appendix 11.

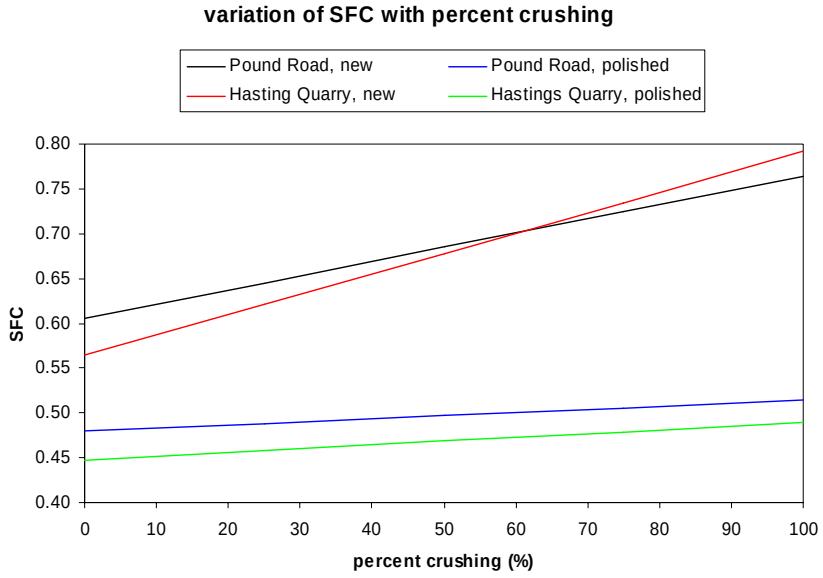

Figure 9.4 Estimated variation of SFC with percent crushing.

9.6 Potential differences in predicted and actual skid resistance

As Equation 9.3 was calibrated purely for laboratory-constructed surfaces, a number of potential differences exist between the predictions given in this Chapter 9 and actual measurements on made on road surfaces. These potential differences are detailed in Appendix 11.

Key observations from Appendix 11 are:

1. The variation in BPN for a doubling of contact area is approximately 3 BPN (Fwa et al. 2003).
2. The variation in BPN for a doubling of aggregate spacing from a gap width of 2.5 mm to 5.0 mm is approximately 2.5 BPN (Fwa et al. 2003).
3. The aggregate from Hastings Quarry used for the tests described in this research report was more irregular in shape than aggregate from Pound Road.
4. The extent to which sharp asperities polish at the junction of crushed-crushed or crushed-uncrushed faces is likely to depend partly on the durability of the aggregate. This may be reflected in tests such as the Aggregate Abrasion Value test (AAV) (BS 812, Part 113:1990).

10. Test procedures for relating skid resistance to percent crushing

10.1 Information required

Four items of information are required to estimate the variation in skid resistance with percent crushing, for a given terminally-polished aggregate:

1. The microtexture of pea-gravel.
2. The microtexture of sealing chip.
3. The shape of pea-gravel.
4. The shape of sealing chip.

No tests are proposed to measure the shape of pea-gravel (item 3) or the shape of sealing chip (item 4) because:

1. for heavily polished surfaces, the part of the macrotexture in contact with HCV tyres is similar whether crushed chip or uncrushed chip is used (i.e. initially sharp edges resulting from crushing become 'rounded' with polishing, Section 9.4);
2. most of the increase in skid resistance with crushing results from introducing additional microtexture (item 2, Table 10.1) rather than increasing chip 'angularity'.

Test methods used to measure the listed items 1-4 are shown in Table 10.1.

Table 10.1 Test methods proposed for measuring parameters required for estimating skid resistance variation.

Item	Parameter	Test Method	Standard
1	Microtexture of pea-gravel	PSV test	BS 812, Part 114:1989
2	Microtexture of sealing chip	PSV test	BS 812, Part 114:1989
3	Shape of pea-gravel	No test method proposed	n/a
4	Shape of sealing chip	No test method proposed	n/a

10.2 Determination of microtexture

Given that measuring the surface profile directly with an instrument such as the Surtronic 3+ does not clearly identify a unique measure of an aggregate's microtexture (Section 6.2), the alternative of using the PSV was chosen.

Two PSV tests are proposed, one for pea-gravel (item 1, Table 10.1), and the other for sealing chip (item 2, Table 10.1).

10.3 Determination of percent crushing

In addition to the four items to be measured (listed in Section 10.1), a test to establish the percent of crushed chips is required.

10.3.1 Initial comments

Transit NZ's existing method for determining the broken faces content of aggregate is set out in the TNZ M/6:2004 specification which states that a minimum of 98% of chips must have at least two broken faces (TNZ 2004). The sample size for this visual test is 120 chips.

For this research, a number of methods have been investigated for determining the percentage of crushed chips including (a) manual techniques where individual broken faces are counted, (b) angularity tests, and (c) automated image-based techniques using cameras.

For this particular application, angularity tests would appear a reasonable choice given that:

- manual techniques can be labour-intensive and time-consuming;
- at the time of writing this report, image-based tests are used for research purposes only, and have not yet reached a stage of development where they are commercially useable.

The results of angularity tests for determining the percentage of crushing are presented in Section 10.3.2.

10.3.2 Angularity tests to determine percent crushing

To predict percentage crushing, angularity tests were carried out according to British Standard BS 812: Part 1:1975, 7.5 *Determination of angularity number*. This Standard was withdrawn in May 1994. The only modification to the procedure outlined in the Standard is that the mass of compacted aggregate (M) was determined rather than the angularity number.

Before testing, the aggregate was sieved, washed, and dried. A total of six determinations were made for each aggregate sample. In total, three aggregate samples were tested.

Results are shown graphically in Figures 10.1 to 10.3. Tables containing numerical data are in Appendix 12.

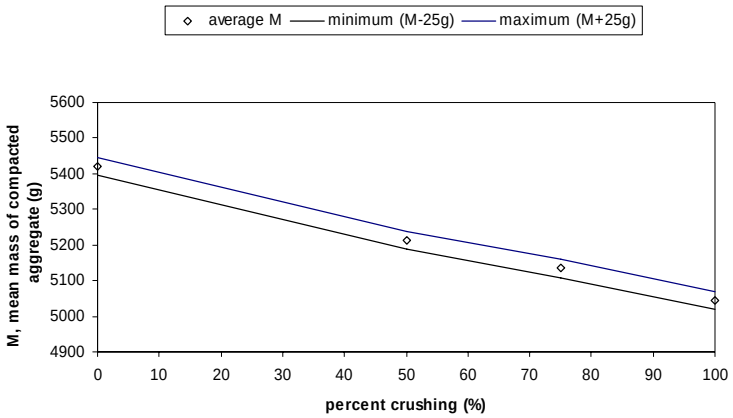

Figure 10.1 Mass of compacted aggregate v percent crushing (Hastings Quarry – pass 9.5 mm sieve, held 6.7 mm sieve).

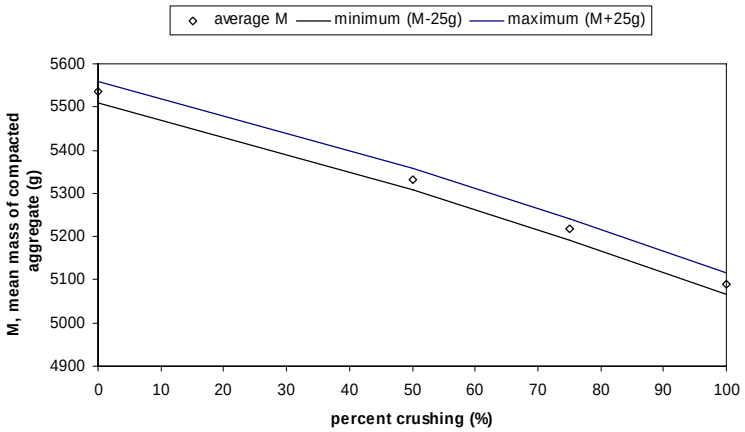

Figure 10.2 Mass of compacted aggregate v percent crushing (Pound Road Quarry – pass 9.5 mm sieve, held 6.7 mm sieve).

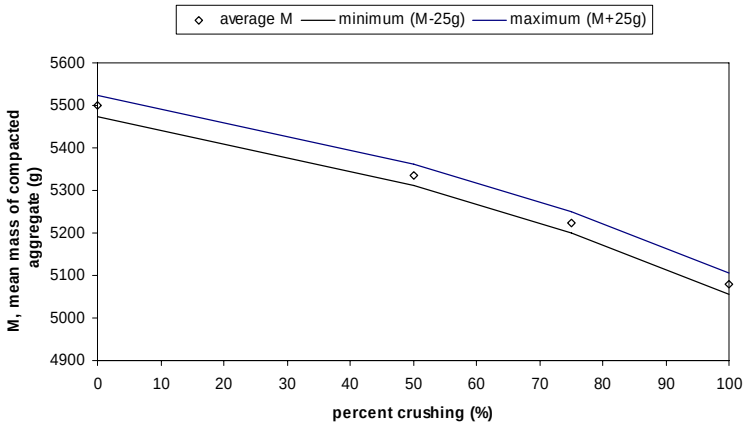

Figure 10.3 Mass of compacted aggregate v percent crushing (Pound Road Quarry – pass 13.2 mm sieve, held 8.0 mm sieve).

According to Figures 10.1-10.3, the percent crushing with tests of this kind can be determined to within 10-15% resolution if the mass of the compacted aggregate is determined within ±25 g of the average in accordance with the Standard. The exact resolution to which percent crushing can be determined depends on (a) the source quarry, and (b) the chip size (i.e. the sieve sizes) as discussed below. Other factors may also affect the prediction, but these have not been investigated as part of this research project.

General observations on the relationship between percent crushing and the mass of compacted aggregate are:

1. The relationship is linear for the range of percent crushing values of interest (say percent crushing > 50%).
2. The relationship varies with source quarry. This may be a function of:
   - Aggregate density (for greywacke, the density is generally around 2680 kg/m^3, but this is likely to vary slightly depending on the exact composition of the aggregate and so is a function of aggregate source);
   - Chip shape (the chip shape is likely to be a function of the unprocessed shape for pea-gravel, and the crushing method for 100% crushed chip);
   - Size and shape distribution of chips (the size and shape distribution of chips will depend on the aggregate source, sizing method, and crushing method).

For percent crushing values greater than 50%, the relationship does not appear to alter with chip size (Figures 10.2 and 10.3).

This test would appear reasonable for determining the percent crushing of aggregate from a particular quarry. Provisos are:

1. The pea-gravel and sealing chip must be similarly sized (i.e. prepared with sieves of the same size);
2. The pea-gravel and sealing chip must be from the same quarry source.

10.4 Predictions

Using Equation 9.3, and ignoring the contribution of chip shape to skid resistance by assuming that the surface is polished to the degree that initially 'sharp' aggregate edges have become 'rounded', and are similar in shape to uncrushed edges, the variation of PSV with percent crushing is given as:

$$PSV = [1 - p] \times PSV_0 + p \times PSV_{100} \qquad \text{Equation 10.1}$$

where:

- p = the proportion of crushed chips (i.e. the percentage of crushed chips divided by 100) (Section 10.3)
- PSV_0 = PSV for 0% crushed chips (Section 10.2)
- PSV_{100} = PSV for 100% crushed chips (Section 10.3)

11. Other test procedures

While the test methods for quantifying aggregate shape described in this chapter are not practical and/or not recommended for implementation, they are of general relevance to this research and have therefore been included.

11.1 Particle shape classification

The three well-accepted methods of classifying particle shape are, in decreasing order of profile feature size: (a) form, (b) roundness, and (c) surface texture. A comprehensive discussion on this classification technique is given by Boggs (1995).

11.2 SHRP angularity test procedures

Ensuring adequate chip angularity is important in hot mix asphalt (HMA) mixes where aggregate particles must have sufficient internal friction to resist permanent deformation (Kennedy et al. 1994). To this end, the Strategic Highway Research Program (SHRP) in the US has developed test procedures for ensuring adequate aggregate angularity. An example is ASTM Standard Method of Test C, 1252, *Uncompacted Void Count of Fine Aggregates*.

11.3 Image-based particle shape classification procedures

As far as the authors of this report are aware, image-based techniques for classifying aggregate particles are used only in research and have not yet been developed to the point where they can be used by commercial laboratories. Generally with image-based techniques, digitised images from one or more cameras are captured and processed to yield information on characteristics of aggregate chips. Most of the research has been carried out over the last 5 years in the US, and some of this research is summarised here.

Bowman et al. (2001) have used electron microscope images to analyse the texture of sand particles. Before segmentation and processing, the images were converted into a digital grey-scale format with analysis relying on Fourier descriptors. The requirement for a scanning electron microscope would rule this approach out for routine tests.

Kuo & Freeman (2000) discuss image indices for characterising aggregates. The indices chosen are summarised in Table 11.1. Predictions using these indices were compared the results of uncompacted void tests.

Table 11.1 Image indices.

Feature	Index
Shape	Aspect ratio (length/width)
Angularity	Perimeter ratio squared (convex/ellipse)
Surface texture	Perimeter ratio squared (actual/convex)

Masad et al. (2000) describe a method of determining fine aggregate angularity using 2-dimensional images. Masad's algorithm is based on (a) image erosion/dilatation, and (b) the fractal[3] technique. Comparisons are made with indirect (i.e. mechanical) test methods for determining uncompacted voids and angle of internal friction. The paper identifies that the indirect mechanical methods are the manifestation of several aggregate characteristics, whereas image-based characterisation techniques are not. Masad also shows that image resolution is important to the predicted angularity.

Rao & Tutumluer (2000) discuss an elegant system employing three orthogonal cameras mounted at the front, top, and to the side of aggregate samples. This system was used to measure aggregate particle weights by determining volumes. Results compared favourably with experimentally determined values.

Maerz (2003) used a rotating table to carry aggregate chips past two cameras: one camera mounted vertically and the other mounted horizontally at aggregate height. The imaging software determined the aggregate profile and used a 'curve radius' method to determine aggregate angularity. Good correlations with mechanical tests were obtained.

Fletcher et al. (2003) describe the initial development of a sophisticated 3-dimensional system for capturing aggregate particle images using video cameras and a video microscope. This system is further described by Chandan et al. (2004) who go on to propose a method for classifying the texture, angularity, and form of aggregate particles. Texture is classified using a black-and-white video camera and video microscope with the wavelet decomposition method. Angularity and form measurements use only the video camera images with angularity being determined by a gradient analysis. For form indices, the shape-factor and sphericity indices are determined using the particle measurements in 3-dimensions. These measurements are determined by controlling the camera's position in 3-dimensions. In a follow-on paper, Masad et al. (2004) compare aggregate shape predictions using conventional and image-analysis methods with respect to HMA performance. In general, results indicated that the image-analysis methods of classifying aggregate shape had a better correlation with HMA performance than conventional methods.

Kim et al. (2004) present a method for classifying aggregates based on size using laser profiler measurements. The profiler collects 3-dimensional data points on particle surfaces. This approach has the advantage that: (a) the aggregates need not be measured separately and can be situated on piles of aggregate, and (b) variations in ambient light are less important than for digital image analysis techniques. The aggregate samples were characterised by wavelet analysis and a neural network.

Wang et al. (2004) present a discussion of a system using x-ray tomography to obtain a 3-dimensional representation of a granular system typical of chipseals and HMA pavements. No analysis of particle classification was attempted, and this equipment would

[3] Fractal – curve or surface generated by some repeated process involving successive definition. Word coined to describe a shape with 'fractional dimension'.

appear to be more sophisticated than is warranted for classifying aggregate particle shape.

Wettimuny & Penumadu (2004) present a Fourier analysis of image shapes to classify aggregates. The paper does not address hardware requirements and purely concentrates on analysis techniques.

11.4 Flow cone tests

Flow cone tests were carried out as part of this research project. It was hoped that time taken for a fixed mass of aggregate to evacuate a cone would increase with inter-particle friction and allow different aggregates to be ranked according to their microtexture. The expectation was that the particle shape (a function of percentage crushing, source quarry, and crushing method) would influence the flow time. Therefore it was envisaged that all tests would be carried out on aggregates with similar macrotextures.

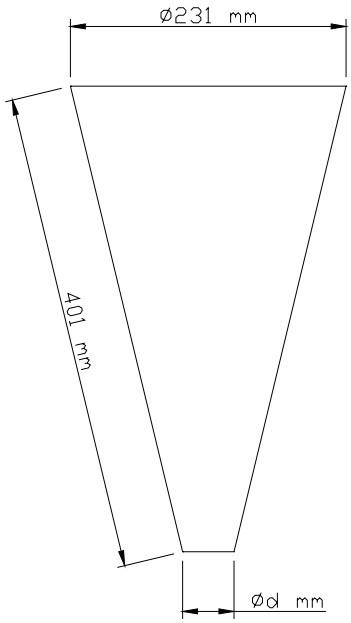

Figure 11.1 Funnel for flow cone tests.

In lieu of formal tests, trials were carried out using a number of cone angles, cone sizes, cone outlet diameters, and hoppers with the aim of maximising flow time and so providing opportunity to distinguish between aggregate microtextures. These initial trials quickly showed that cone outlet diameter (Ød, Figure 11.1) was critical. If the cone outlet diameter was too small then the flow would stop intermittently because of aggregate blockage, and if the cone outlet diameter was too large, flow was rapid and accurate timing was difficult.

Table A14.1 in Appendix 14 shows the results of some of the trials with the funnel illustrated in Figure 11.1.

The trials were carried out on the following aggregate:

Aggregate Source:	Hastings Quarry
Crushing:	Sealing chip
Sieve:	Pass 9.5 mm, held 6.7 mm
Aggregate Mass:	9000 g
Aggregate Preparation:	Washed in water and dried

The aggregate was chosen to be relatively small in size (pass 9.5 mm sieve, held 6.7 mm sieve) as this allowed a smaller cone outlet diameter, reduced equipment bulk, and reduced the required mass of aggregate for testing.

This test method was eventually abandoned because a cone outlet diameter of sufficient size that would not block resulted in rapid cone evacuation times that could not be timed with sufficient accuracy to differentiate aggregates. This test is not therefore recommended for further development.

11.5 Determination of macrotexture of existing roads using the SLP

Supplementary tests were undertaken with Transit NZ's SLP to determine if the percentage of crushed chips could be determined for chipseal surfaces on the road. It was hoped that information from such tests, along with RAMM information, would allow a relationship between the broken faces content of chipseal surfaces and skid resistance to be established. While this technique showed that the percentage of crushed chips could be determined, the resolution with which this could be done was not sufficiently fine to be useful.

SLP measurements were measured on the 15 laboratory prepared plates (300 mm x 150 mm) with known percentages of crushed/uncrushed chip. SLP profile scans were parallel and spaced 2 mm apart with an average of 55 scans being made on each plate. Plate images are shown in Appendix 1 and analysis detail in Appendix 5.

Five methods were used in the attempt to predict the percent crushing from macrotexture profile SLP measurements. These methods are summarised in Table 11.2.

The figures in Appendix 5 show that correlations between the actual percentage of crushing and the trends predicted by each of the 5 methods listed in Table 11.2 are not sufficiently accurate to be useable. While trends would be expected to improve for a greater number of scans, this would not be economic and is not therefore a realistic option. Some reasons for the relatively weak and variable trends between SLP profile characteristics and the percent of crushed chips include:

1. Some uncrushed faces are essentially straight.
2. The corners of crushed-uncrushed faces may be similarly sharp to crushed-crushed faces.
3. The sealing chip and pea-gravel was not sieved before combination and therefore the size and distribution of aggregate of a particular grade may not be the same.

Table 11.2 Methods for predicting the percent crushing from SLP profiles.

Method	Description
1	Correlation of percent crushing with the profile statistics.
2	Correlation of a linear approximation to the profile with the actual profile. (The actual profile was approximated by straight lines with the assumption that crushed faces would be predominantly 'straight', and uncrushed alluvial faces 'curved'. Correlations between the actual profile and the straight line approximation would thus be higher for surfaces with a higher percent of crushed aggregate.)
3	Representing smooth 'curved' faces by 2nd-order polynomials (i.e. quadratics) and assuming that these faces were uncrushed. (The remaining 'irregular' faces were assumed to be crushed, and correlation between these 'crushed faces' and the actual profile was calculated – correlations being higher for surfaces with a higher percent of crushed aggregate.)
4	Comparison of PSDs of the SLP profiles for different percentages of crushed aggregate. (The intention was that the 'ragged' profile of newly crushed faces could be distinguished from relatively smooth uncrushed faces by comparing PSDs at short wavelengths of less than 1 mm.)
5	Comparison of PSDs of the SLP slope profiles for different percentages of crushed aggregate. (It was thought that abrupt changes of slope would occur at the interface between crushed-crushed and crushed-uncrushed faces, and this would be reflected in a greater magnitude of slope PSD of crushed chips at short wavelengths.)

In addition, SLP profiles from actual road sites could be expected to show less variation with percent crushing than the unpolished laboratory samples for the following reasons:

1. The sharp edges at the interface between crushed-crushed and crushed-uncrushed faces can become rounded because the polishing action of vehicle tyres makes them harder to distinguish from uncrushed faces.
2. The bitumen level in chipseals can be high, particularly for flushed surfaces, leaving little exposed aggregate for distinguishing the percentage of crushed chips based on SLP profile measurements.

Generally, the percentage of crushed aggregate in roads is greater than 70%, with much higher percentages occurring for recently laid chipseal surfaces. (TNZ M/6:2004 specification requires that at least 98% of aggregate chips have two or more broken faces.) Predicting the actual percentage of crushed faces from SLP profiles with an accuracy that would be useful would be difficult.

12. Conclusions and recommendations

12.1 Conclusions

The results of PSV, GripTester and BPT tests on core samples and laboratory-prepared chipseal surfaces from two quarries using greywacke indicate that:

- Skid resistance increases linearly with percentage crushing. For new and unpolished aggregate, the increase in BPN in going from 0% crushed chips to 100% crushed chips is approximately 25%.
- Skid resistance increases with crushing by two mechanisms:
  - The microtexture of crushed faces is greater than the microtexture of uncrushed faces (the increase in PSV of crushed faces compared with uncrushed faces is approximately 4.5 PSV units).
  - New and unpolished crushed chips are more 'angular' in shape than uncrushed chips, but for heavily polished surfaces where sharp chip edges have become rounded, the increase in BPN related to chip shape in going from 0% crushed chips to 100% crushed chips is estimated as negligible.
- The increase in skid resistance caused by crushing mainly results from (a) the increased microtexture of crushed faces rather than (b) the 'angular' shape of crushed chips (e.g. for new and unpolished chip, the increase in BPN in going from 0% to 100% crushed chips is 19% related to microtexture increases, and 7% related to increases chip shape 'angularity').
- BPN is not noticeably affected by chip size (i.e. chip grade).
- The degree of crushing required to meet a particular level of skid resistance depends both on uncrushed and crushed (a) microtexture, and on (b) chip shape.
- Aggregates with a lower level of microtexture need to be crushed more to achieve a given level of skid resistance (e.g. new and unpolished aggregate with a PSV of 55 needs 100% crushed chips to achieve the same skid resistance as aggregate with a PSV of 57 that has 88% crushed chips). (Skid resistance is measured by GripNumber in 'push' mode, i.e. GN´.)
- For aggregates with the same microtexture, chips that have 'irregular' shapes have a greater BPN than 'round' chips (e.g. when 100% crushed, the BPN of 'irregular' chips is greater than that of 'rounded' chips by approximately 9 BPN).
- The benefit of crushing on skid resistance is greater for new and unpolished chipseal surfaces than for terminally-polished chipseal surfaces. Polishing reduces the benefit of crushing on skid resistance by (a) reducing the microtexture of crushed faces, and (b) 'smoothing' sharp chip edges that were angular when first produced.

- The beneficial effect of crushing on microtexture remains after the equilibrium level of polish is achieved. (The increase in PSV when 100% crushed chips are used instead of 0% crushed chips is between 10 and 15 for unpolished chips, but this reduces to between 4 and 5 PSV after PSV polishing.)
- Sharp or angular asperities at the edges of chip faces on new and unpolished chip become rounded with polishing by HCVs.
- When operated on low-friction surfaces, the GripTester in 'push' mode gives different trends of skid resistance than the BPT.
- The test specified by the British Standard *Determination of angularity number* (BS 812: Part 1:1975, 7.5) would appear useful for determining the percentage of crushed chips. (Such a test may also be useful for quantifying chip shape, although this has not been investigated as part of this research.)

12.2 Recommendations

- Further develop and validate the conclusions above using:
  - aggregate from additional quarries;
  - on-road skid resistance measurements using the GripTester in 'tow' mode on a range of specifically constructed chipseal surfaces with a range of percentage of crushed chips (e.g. 0%, 50%, 80%, and 100%).
- Further investigate the test method of BS 812: Part 1:1975, 7.5 to quantify the shape of aggregate chips and so enable the contribution of chip shape to skid resistance to be accurately predicted.
- A survey of crushing methods employed by New Zealand sealing chip suppliers should be undertaken. This survey should aim to determine how the method of crushing (e.g. Barmac, Cone, etc.) affects aggregate shape.

12.3 Analysis technique limitations

- Analysis of the microtexture profiles of aggregate measured using an instrument such as the stylus-based Surtronic 3+ has not been useful in this research.
- It has not been possible in this research to accurately compare the polishing employed in the PSV test with actual polishing of tyres on the road. Consequently, it has not been possible to validate (or otherwise) the polishing action employed in the PSV test.
- It has not been possible in this research to distinguish the percentage of crushed faces in existing surfaces with analysis of Stationary Laser Profiler (SLP) profiles.
- Image-based shape classification techniques at the time of preparing this report are useful only as research tools and have not been developed to the point where they can be used in laboratory test procedures.

13. References

Anderson, D.A,, Henry. J.J. 1979. The selection of aggregates for skid resistant pavements. *Proceedings, Association of Asphalt Paving Technologists, Technical Sessions*, Denver Colorado, pp. 587-610.

Boggs, S. Jr. 1995. *Principles of sedimentology and stratigraphy*. 2nd edition. Englewood Cliffs. New Jersey: Prentice Hall. 774 pp.

Bowman, E.T., Soga K., Drummond, W. 2001. Particle shape characterisation using fourier descriptor analysis. *Géotechnique 51(6):* 545-554.

Cenek, P.D., Fong, S., Stevenson, H.S., Brown, D.N., Stewart, P.F. 1998. Skid resistance: the influence of alluvial aggregate size and shape. *Transfund New Zealand Research Report No. 119.* 100 pp.

Cenek, P.D., Carpenter, P., Jamieson, N., Stewart, P. 2004. Prediction of skid resistance performance of chipseal roads. *Transfund New Zealand Research Report No. 256.* 114 pp.

Chandan, C., Sivakumar, K., Masad, E., Fletcher, T. 2004. Application of imaging techniques to geometry analysis of aggregate particles. *Journal of Computing in Civil Engineering, ASCE, 18(1):* 75-82.

Choubane, B., Holzschuher, C.R., Gokhale, S. 2004. Precision of locked-wheel testers for measurement of roadway surface friction characteristics. *Transportation Research Record 1869:* 145-151.

Clark, S.K. (Ed.) 1981. *Mechanics of pneumatic tires*. US Department of Transportation, National Highway Traffic Safety Administration, Washington DC 20590.

French, T. 1989. *Tyre technology*. Adam-Hilger, Bristol and New York. 170 pp.

Fletcher, T., Chandan, C., Masad, E., Sivakumar, K. 2003. Aggregate imaging system for characterizing the shape of fine and coarse aggregates. *Transportation Research Record 1832, Paper No. 03-2174:* 67-77.

Fong, S. 1998. Tyre noise predictions from computed road surface texture-induced contact pressure. *Internoise 1998*. 4pp.

Fookes, P.G., Lay, J., Sims, I., Smith, M.R., West, G. 2001. *Aggregates: sand, gravel and crushed rock aggregates for construction purposes.* 3rd edition. Smith, M.R. & Collis, The Geographical Society, London. 339 pp.

Fwa, T.F., Choo, T.S., Liu, Y. 2003. Effect of aggregate spacing on skid resistance of asphalt pavement. *Journal of Transportation Engineering. ASCE,* July /August: 420-426.

Horne, W.B., Buhlmann, F. 1981. A method for rating the skid resistance and micro/macrotexture characteristics of wet pavements. *Frictional interaction of Tyre and Pavement,* Meyer & Waler (Editors). *American Society for Testing and Materials, STP 793:* 191-218.

Kennedy, W.T., Huber, G.A., Harrigan, E.T., Cominsky, R.J., Hughes, C.S., Von Quintus, H., Moulthrop, J.S. 1994. Superior performing asphalts (Superpave): the product of the SHRP Asphalt Research Program. *Program SHRP A-410.* Strategic Highway Research, National Research Council, Washington DC.

Kim, H., Rauch, A.F., Haas, C.T. 2004. Automated quality assessment of stone aggregates based on laser imaging and a neural network. *Journal of Computing in Civil Engineering, ASCE, 18(1):* 58-64.

Kuo, Chun-Yi, Freeman, R.B. 2000. Imaging indices for quantification of shape, angularity, and surface texture of aggregates. *Transportation Research Record 1721, Paper No. 00-0686:* 57-65.

Liu, Y., Fwa, T.F., Choo, Y.S. 2004. Effect of surface macrotexture on skid resistance measurements by the British Pendulum Test. *ASTM Journal of Testing and Evaluation 32(4),* July.

McDaniel, R.S., Coree, B.J. 2003. Identification of laboratory techniques to optimize Superpave HMA surface friction characteristics – Phase I: Final Report. *SQDH 2003-6, HL 2003-19*, Iowa Department of Transportation. 35 pp.

Maerz, N.H. 2003. Technical and computational aspects of the measurement of aggregate shape by digital image analysis. *Journal of Computing in Civil Engineering, ASCE, 18(1):* 10-18.

Masad, E., Button, J.W., Papagiannakis, T. 2000. Fine-aggregate angularity. *Transportation Research Record 1721, Paper No. 00-0691:* 66-72.

Masad, E., Little, D., Sukhwani, R. 2004. Sensitivity of HMA performance to aggregate shape measured using conventional and image analysis methods. *Road Materials and Pavement Design 5(4):* 477-498.

Minnesota Department of Transportation. 2003. Office of Materials and Road Research, *Laboratory Test Method 1214, Percent Crushed Particles (*Updated May 1 2003), 395 John Ireland Boulevard. *(http://www.mrr.dot.state.mn.us/materials/manual/1214.pdf)*

Mooney, S., Wood, W. 1996. Locked wheel braking in shallow water. *Society of Automotive Engineers, SAE Paper 960653:* 51-68.

Moore, D.F. 1975. *The friction of pneumatic tyres.* Elsevier Scientific Publishing Company.

Perry, M., Woodside, R., Woodward, W. 2001. Observations on aspects of skid-resistance of greywacke aggregate. *Quarterly Journal of Engineering Geology and Hydrology 24:* 347-352.

PIARC Technical Committee on Surface Characteristics C1. 1995. International PIARC experiment to compare and harmonize texture and skid resistance measurements.

Rao, C., Tutumluer, E. 2000. Determination of volume of aggregates: new image-analysis approach. *Transportation Research Record 1721*, *Paper No. 00-1345:* 73-80.

Taylor Hobson. 1993. Surtronic 3+ Operators Handbook. *THP-HB-103. Taylor Hobson Pneumo.* Leicester LE4 9j8. England. 54 pp.

The Encylopaedia Britannica, 11th ed. 2005. Courtesy of "Wikipedia - the Free Encyclopaedia", *http://en.wikipedia.org/wiki/1911_Encyclop%E6dia_Britannica*

Transit New Zealand. 2004. *Suppliers of surfacing aggregate – Polished Stone Value.* Wall Chart September 2004, Transit NZ, Wellington, New Zealand.

Transit New Zealand. 2004. Specification for sealing chip. *TNZ M/6:2004.* 4 pp.

Wang, L.B., Frost, J.D., Lai, J.S. 2004. Three-dimensional digital representation of granular material microstructure from x-ray tomography imaging. *Journal of Computing in Civil Engineering*, *ASCE*, *18(1):* 28-35.

Wettimuny, R., Penumadu, D. 2004. Application of Fourier analysis to digital imaging for particle shape analysis. *Journal of Computing in Civil Engineering*, *ASCE*, *18(1):* 2-9.

Standards

ASME B46.1:1985 *Surface texture (roughness, waviness, and lay)*

ASME B46.1:1995 *Surface texture (roughness, waviness, and lay)*

ASTM E-1960-98 *Standard practice for calculating International Friction Index of a pavement surface*

ASTM 1252 1993 *Standard method of Test C, Uncompacted void count of fine aggregates*

BS 598, Part 105:2000 *Sampling and examination of bituminous mixtures for roads and other paved areas – Methods of test for the determination of texture depth*

BS 812, Part 1:1975 *Testing of aggregate sieve analysis*

BS 812, Part 113:1990 *Testing aggregates. Method for determination of aggregate abrasion value (AAV)*

BS 812, Part 114:1989 *Testing aggregates. Method for determination of the polished-stone value*

BS 7941, Part 1:1999 *Surface friction of pavements - Methods for measuring the skid resistance of pavement surfaces: Side-way force coefficient routine investigation machine*

BS EN 13036, Part 4:2003 *Road and airfield surface characteristics. Test methods. Method for measurement of slip/skid resistance of a surface. The pendulum test*

ISO 4287/1:1984 *Geometrical Product Specifications (GPS) - Surface texture: Profile method – Terms, definitions and surface texture parameters* [replaced by ISO 4287:1997, below]

ISO 4287:1997 *Geometrical Product Specifications (GPS) – Surface texture: Profile method – Terms, definitions and surface texture parameters*

ISO 13473-1:1996 *Characterization of pavement texture by use of surface profiles – Part 1: Determination of Mean Profile Depth*

ISO 13565-1:1996 *Geometrical Product Specifications (GPS) - Surface texture: Profile method; Surfaces having stratified functional properties - Part 1: Filtering and general measurement conditions*

ISO 13565-2:1996 *Geometrical Product Specifications (GPS) – Surface texture: Profile method; Surfaces having stratified functional properties – Part 2: Height characterization using the linear material ratio curve*

TNZ M/6:2004 *Notes on specification for sealing chip*